MEASUREMENT OF CROSS-SECTIONS FOR TRANSFER OF EXCITATION

SENSITIZED FLUORESCENCE IN CAESIUM VAPOUR

A thesis submitted as a requirement for the degree of Master of Science based on work carried out in the Department of Physics of the School of General Studies, Australian National University by

MERVYN HAROLD DOOBOV

Canberra, August 1969

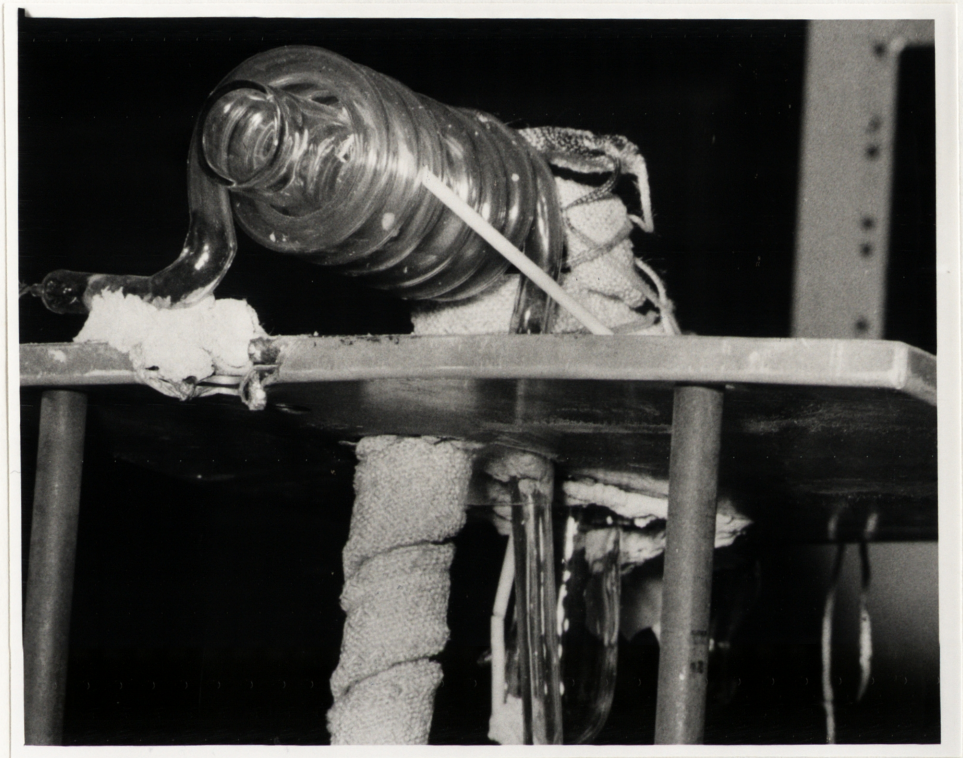

View of Resonance Cell and Helium Lamp

ABSTRACT

Sensitized fluorescence arising from the optical excitation of caesium atoms to the $8^2P_{1/2}$ level by helium light is investigated. It is found that the $8^2P_{3/2}$, $7^2D_{3/2}$, and probably the $7^2D_{5/2}$ levels are populated through collisions of the second kind with inert gas atoms, the dominant process path being

$$8^2P_{1/2} \rightleftarrows 8^2P_{3/2} \rightleftarrows 7^2D_{3/2} \rightleftarrows 7^2D_{5/2}$$

The cross-sections for the first two of these processes are found to be for $Q_{12}(8P_{1/2} \rightarrow 8P_{3/2})$, $Q_{21}(8P_{3/2} \rightarrow 8P_{1/2})$, $Q_{23}(8P_{3/2} \rightarrow 7D_{3/2})$, and $Q_{32}(7D_{3/2} \rightarrow 8P_{3/2})$ respectively: 20, 20, 13, and 3.3 $\mathring{A}^2$ for Cs-He collisions (experimental run 1); 40, 40, 16, and 3.9 $\mathring{A}^2$ for Cs-He (experimental run 2); 6, 6, 35, and 11 $\mathring{A}^2$ for Cs-A; 12, 3, 39, and 8 $\mathring{A}^2$ for Cs-Kr (experimental run 1); and 19, 13, 57, and 26 $\mathring{A}^2$ for Cs-Kr (experimental run 2).

The results are found to correlate with the elastic scattering cross-sections for electron-inert gas collisions, the electron energy taken to be the same as the electron in the $8P_{1/2}$ state of caesium. The results also confirm Winans' partial selection rule for sensitized fluorescence.

CONTENTS

LIST OF FIGURES

LIST OF TABLES

ACKNOWLEDGEMENTS

While it is not possible to mention all those who have contributed in some way to this project, I wish particularly to express my gratitude to my supervisor, Dr. L.O. Brown, who suggested it. His helpful advice and discussions concerning the project were no small factors in its completion. I wish also to thank Dr. M. Andrews who wrote the computer programs.

I gratefully acknowledge the assistance of the Australian National University in the form of a Master's Degree Scholarship and for providing the necessary facilities.

It is not possible to overestimate the encouragement of my wife, Sue, who has also typed this thesis.

Unless otherwise acknowledged, the work described in this report was carried out by the author.

M Doobov

M. DOOBOV

1. INTRODUCTION

1.1 EARLY WORK

It was demonstrated by Boeckner[1] (1930) that one could excite atoms in caesium vapour to the $8\,^2P_{1/2}$ level by irradiation with light from a helium discharge. This is possible because of the fortuitous overlapping of the lines due to the $8\,^2P_{1/2} - 6\,^2S_{1/2}$ transition in caesium and to the $3\,^3P - 2\,^3S_1$ transitions in helium both of which have a wavelength of 3889 Å. The coincidence is shown in Figure 1.1 while the detailed line-shapes are shown in Figure 1.2.

Boeckner found that the relative intensities of the lines due to the transitions $8\,^2P_{1/2} \rightarrow 6\,^2S_{1/2}$ and $8\,^2P_{3/2} \rightarrow 6\,^2S_{1/2}$ were 10 and 0 respectively; with 0.6 torr of helium present they were 4 and 2; with 4 torr of helium, they were 2 and 4. He deduced that excitation was transferred from the $8\,^2P_{1/2}$ level to the $8\,^2P_{3/2}$ level and the $7\,^2D$ levels during collisions of the second kind. These levels are respectively 82 cm^{-1} and 350 cm^{-1} higher than the $8\,^2P_{1/2}$ level. Boeckner further concluded that excitation transfer to other levels is unlikely.

Fig. 1.1 - Caesium and Helium Spectra.
(Taken on Ilford Long Range Spectrum Plate through a Hilger & Watts Constant Deviation Spectrometer. Exposure times are shown.)

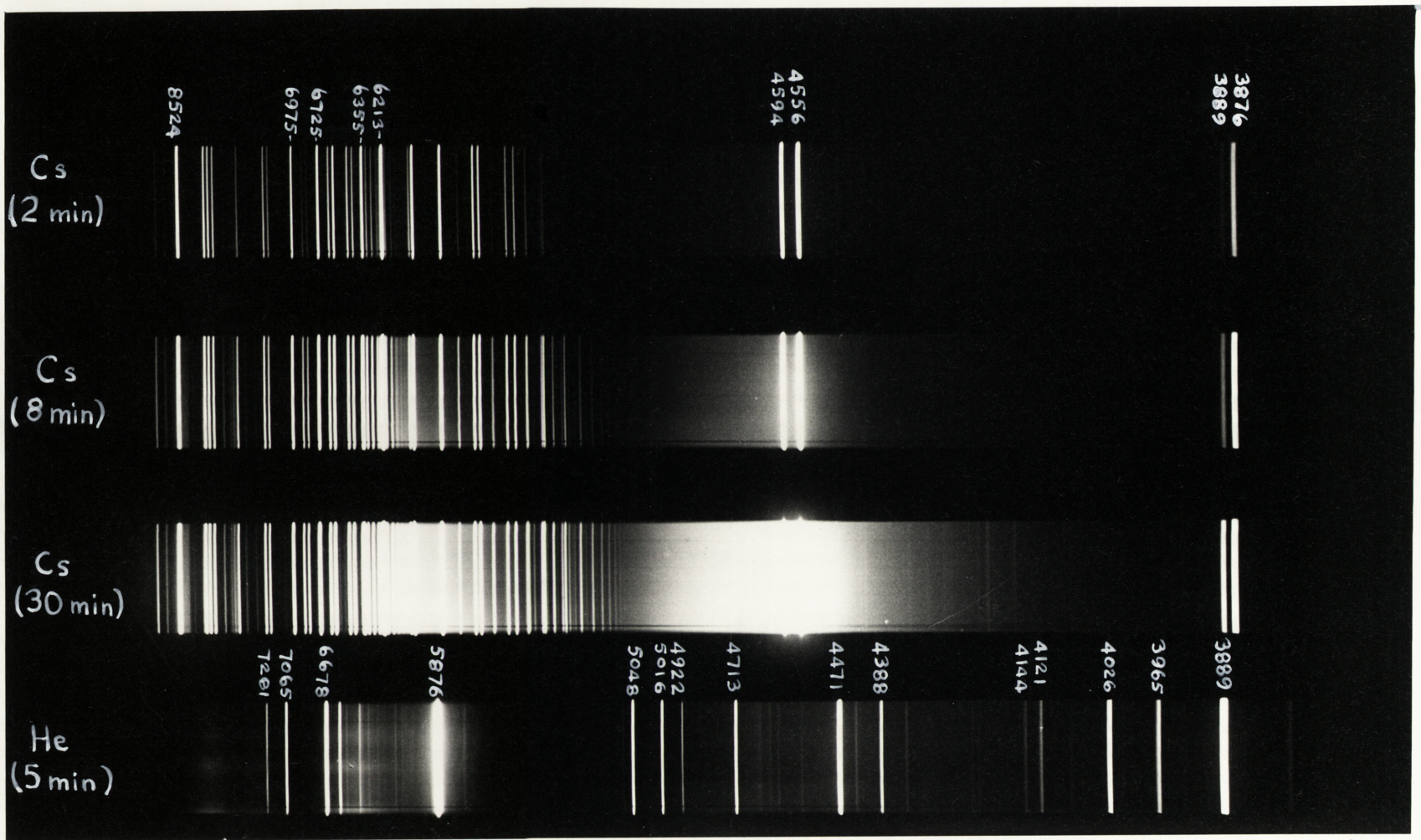

Fig. 1.1 - Caesium and Helium Spectra

$$^{*}\frac{\Delta\lambda}{\lambda} = \frac{2}{\epsilon_N}\sqrt{\frac{2RT\ln 2}{M}} = 1.38\times10^{-6} \text{ for Cs}$$

$$T = 500^{\circ}K$$

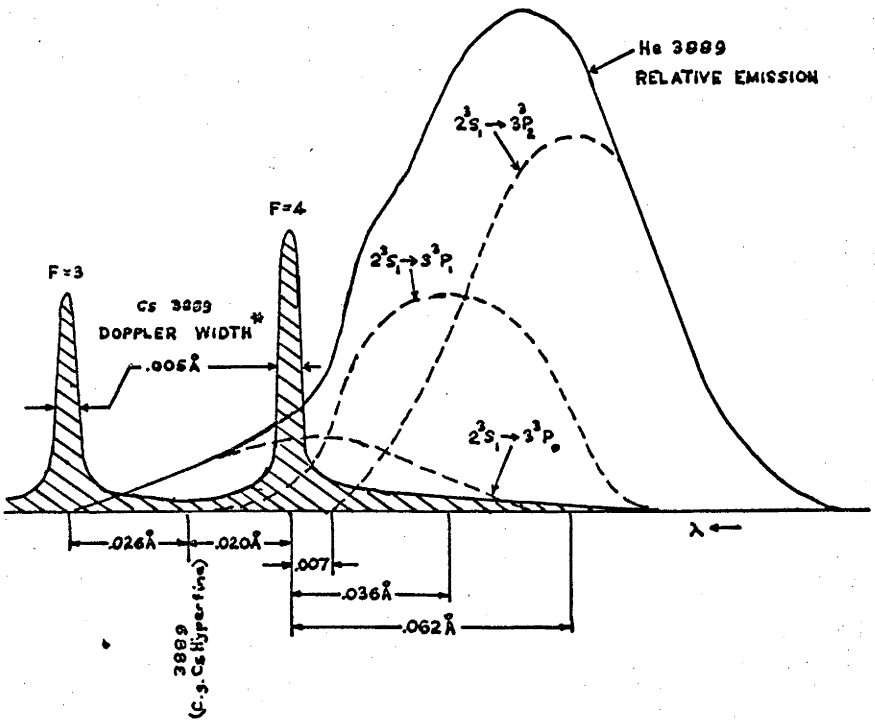

Fig 1.2 He & Cs 3889 Lineshapes [7]

1.2 SENSITIZED FLUORESCENCE

The extra energy required in the excitation transfer processes described above comes from the kinetic energy of the colliding atoms (at 79°K the mean kinetic energy of a gas is 82 cm^{-1}; at 335°K it is 350 cm^{-1}). The lower energy levels of caesium which are concerned in these processes are shown in Figure 1.3.

The process, by which an excited atom gives up its excitation energy during an inelastic collision of the second kind to another atom (with either liberation or absorption of kinetic energy) which later emits radiation, is known as sensitized fluorescence. The normal process, by which the originally excited atom emits radiation of the same wavelength as the exciting radiation and thereby returns directly to the ground state, is known as resonance fluorescence. See for example, Mitchell and Zemansky[3].

1.3 RECENT WORK

The coincidence of the spectral lines has been used to excite the caesium laser which is, so far, the only optically pumped gas laser[2]. Gould[7]

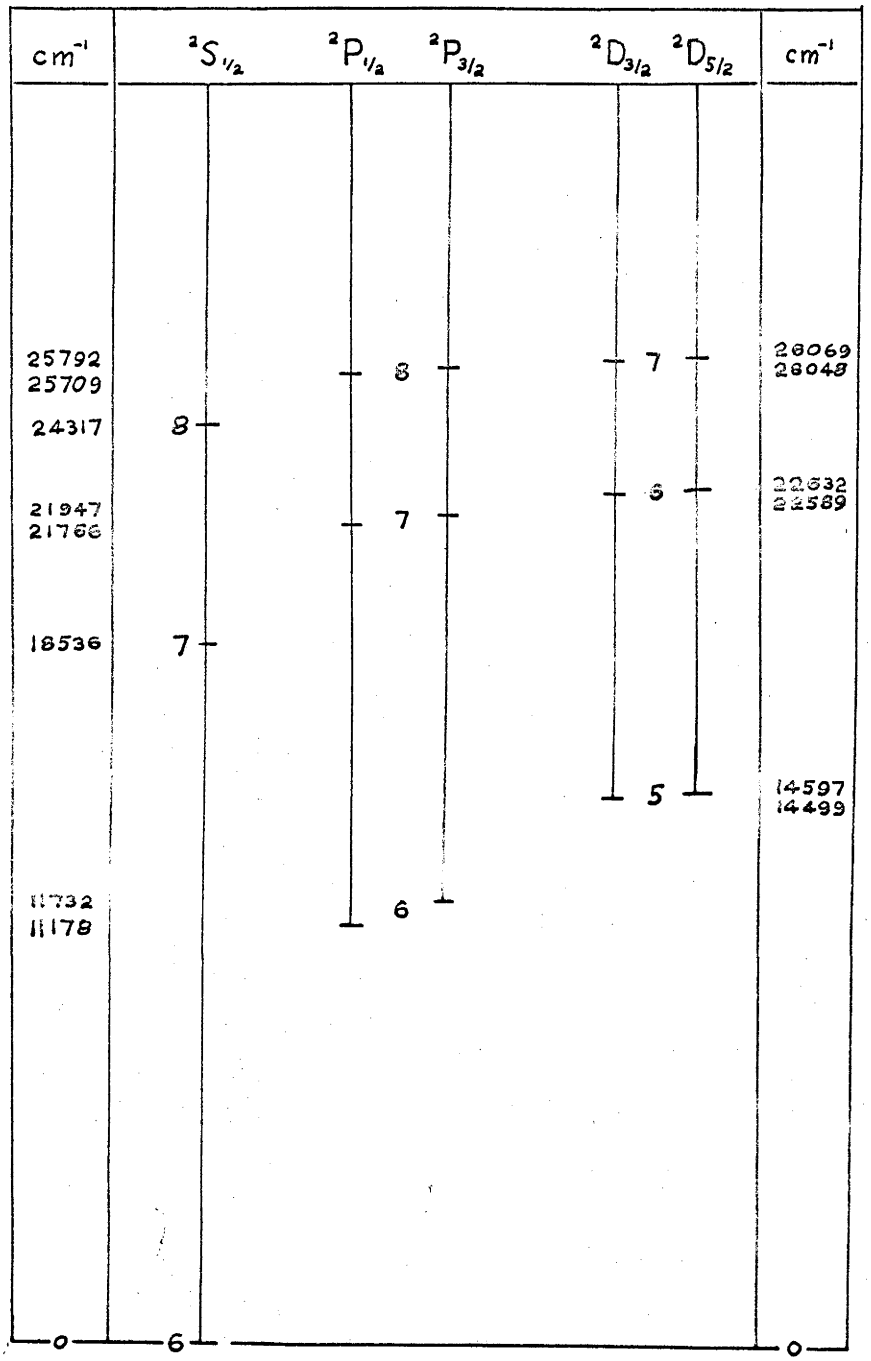

Fig. 1.3 - Cs Energy Levels

states only 0.1% of the output of a helium lamp is emitted as the 3889 Å line and that, further, only 1% of the helium line is absorbed by caesium vapour (see Figure 1.2).

In a recent series of experiments, Krause and co-workers have investigated sensitized fluorescence in alkali vapours including the quenching effects of inert gases[4]. They have also investigated the effects on collisions in caesium vapour of gases such as nitrogen, hydrogen, HD, and D_2 molecules[5].

Krause used the conventional technique of irradiating the alkali vapour with one of the D-lines and measuring the intensities of both the resonance and sensitized fluorescence lines whose ratio, together with the ratio obtained by irradiating with the other D-line, yields the cross-section of the excitation transfer process. In every case the lowest ^2P levels were excited.

In order that radiation trapping not influence the results, Krause used a specially designed resonance cell in which the exciting radiation after passing through a front window just grazes an inside wall. Fluorescence was monitored at right angles

to the exciting beam through a side window in this wall near the front window. Radiation then passes through only a thin layer of unexcited atoms. Further, the experiments were restricted to low alkali vapour pressures ($<\sim 10^{-5}$ torr).

More recently, Gallagher[13] has carried out experiments involving excitation transfer in rubidium and caesium using a technique similar to that of Krause. By measuring values of the cross-section at various temperatures, Gallagher was able to estimate the actual cross-section (the measured cross-section being an average of the actual cross-section over the thermal inter-atomic velocity distribution). Gallagher measured cross-sections for collisions with inert gases.

1.4 RADIATION TRAPPING

The light emitted in a radiative transition from an excited state to the ground state has a high probability of being re-absorbed by another atom in the ground state. After an average period of one lifetime, the newly excited atom will re-emit a photon which may be again re-absorbed and so on. This process is known as radiation trapping or imprison-

ment of radiation or resonance trapping. Its effect is to increase the apparent lifetime of the excited state.

If the excited state concerned is not the lowest excited state there is a probability that the radiation emitted is not resonance radiation. This radiation will not be subject to resonance trapping so that the associated rate of decay will not be apparently decreased.

Theoretical treatments have been devised to allow for radiation trapping. Most treatments such as that of Holstein[6] treat the problem as one of diffusion of photons through the gas. The calculations involved in solving the equations are difficult and the reliability of the results is not very great. Hence Krause and Gallagher chose to work at low vapour pressures where radiation trapping effects are negligible.

1.5 PRESENT INVESTIGATION

The aim of the present investigation is to measure the cross-sections for transfer of excitation between the $8\,^2P_{1/2}$ and $8\,^2P_{3/2}$ levels of caesium during collisions of the second kind. The cross-sections

for the same excitation transfers during collisions of excited caesium atoms with inert gas atoms (helium, argon, and krypton) are also to be measured.

The caesium is to be excited to the $8\,^2P_{1/2}$ level by irradiation with helium light. By measuring the ratio of the intensities of radiation in the lines 8921 Å ($8\,^2P_{1/2} - 5\,^2D_{3/2}$) and 8933 Å ($8\,^2P_{3/2} - 5\,^2D_{5/2}$) and determining its variation with caesium vapour pressure in the former case (inert gas pressure in the latter case) it should be possible to deduce the cross-sections.

Since the radiation to be measured is not resonance radiation, it will not be necessary to allow for radiation trapping as this will not affect the observed lines.

2. THEORY

2.1 PROCESS

The process considered is a chain of simple reactions. Caesium atoms in the ground ($6S_{1/2}$) state are irradiated with helium light, the 3889 Å component of which causes some of the atoms to be excited to the $8P_{1/2}$ level. (The superscript representing the multiplicity of caesium energy levels is always two and will be omitted since no confusion can arise.):

$$Cs(6S_{1/2}) + \text{light } (3889\ \text{Å}) \rightarrow Cs(8P_{1/2}) \quad (2.1)$$

Some of these excited atoms can be further excited by collisions of the second kind with another caesium atom or with an atom of inert gas which may be present.

$$Cs(8P_{1/2}) + A + \Delta E \rightleftarrows Cs(8P_{3/2}) + A \quad (2.2)$$

A represents either another caesium atom or an atom of inert gas. ΔE is the energy taken from or given up to the kinetic energy of the atoms and is equal to the difference of the energies of the two levels concerned. ($\Delta E = 82.64\ cm^{-1}$) (8)

It will be assumed that the number of excited caesium atoms at any time is much less than the total

number of caesium atoms. Hence the number of unexcited caesium atoms may be put equal to the total number of caesium atoms. (It also follows that collisions between two excited caesium atoms are so rare as to be able to be neglected.)

Caesium atoms in the $8P_{3/2}$ state may be further excited in collisions of the second kind to the $7D_{3/2}$ level and thence through even further collisions to the $7D_{5/2}$ level:

$$Cs(8P_{3/2}) + A + \Delta E' \rightleftarrows Cs(7D_{3/2}) + A \qquad (2.3)$$

$$Cs(7D_{3/2}) + A + \Delta E'' \rightleftarrows Cs(7D_{5/2}) + A \qquad (2.4)$$

$\Delta E'$ and $\Delta E''$ are the energy defects between the $8P_{3/2}$ and $7D_{3/2}$ levels and the $7D_{3/2}$ and $7D_{5/2}$ levels respectively. ($\Delta E' = 256.08\ cm^{-1}$, $\Delta E'' = 20.97\ cm^{-1}$) [8]

Radiative transitions may occur from each of the excited states:

$$Cs(8P_{1/2}) \rightarrow Cs(\text{lower states}) + (\text{light}) \qquad (2.5)$$

$$Cs(8P_{3/2}) \rightarrow Cs(\text{lower states}) + (\text{light}) \qquad (2.6)$$

$$Cs(7D_{3/2}) \rightarrow Cs(\text{lower states}) + (\text{light}) \qquad (2.7)$$

$$Cs(7D_{5/2}) \rightarrow Cs(\text{lower states}) + (\text{light}) \qquad (2.8)$$

It is assumed that radiative transitions from the 7D levels to the 8P levels are negligible since in each case the branching ratio is less than one percent.

(See Appendix I)

Thus, in this process, ground-state caesium atoms are radiatively and collisionally excited to various levels whence they decay eventually to the ground state either by emitting radiation or through a combination of radiative and collisional processes. The input of light at 3889 Å is equal to the output at various wavelengths (as can be shown from the rate equations to be derived in the following section).

2.2 RATE EQUATIONS

The energy levels $6S_{1/2}$, $8P_{1/2}$, $8P_{3/2}$, $7D_{3/2}$, and $7D_{5/2}$ will be represented by the subscripts 0, 1, 2, 3, and 4 respectively. n_i is the population density of state i. The number density of atomsof inert gas will be denoted by a. The rate constants will be denoted by K_{ij} in the case of caesium-caesium collisions and by k_{ij} in the case of caesium-inert gas collisions. In the case of radiative transitions, the rate constants will have only a single subscript e.g. k_i. The definition of the rate constants will be evident from the rate equations to be derived.

Keeping in mind the assumptions of the previous

section, the rate equations can be written directly from equations (2.1), (2.2), (2.3), (2.4), (2.5), (2.6), (2.7), and (2.8). If steady-state conditions are assumed, the rate equations are:

$$\frac{dn_1}{dt} = k_0 n_0 + (k_{21} a + K_{21} n_0) n_2 - (k_1 + k_{12} a + K_{12} n_0) n_1 = 0 \qquad (2.9)$$

$$\frac{dn_2}{dt} = (k_{12} a + K_{12} n_0) n_1 - \{k_2 + (k_{21} + k_{23}) a + (K_{21} + K_{23}) n_0\} n_2 + (k_{32} a + K_{32} n_0) n_3 = 0 \qquad (2.10)$$

$$\frac{dn_3}{dt} = (k_{23} a + K_{23} n_0) n_2 - \{k_3 + (k_{32} + k_{34}) a + (K_{32} + k_{34}) n_0\} n_3 + (k_{43} a + K_{43} n_0) n_4 = 0 \qquad (2.11)$$

$$\frac{dn_4}{dt} = (k_{34} a + K_{34} n_0) n_3 - (k_4 + k_{43} + K_{43} n_0) n_4 = 0 \qquad (2.12)$$

These equations can be written the matrix form:

$$AN = H \qquad (2.13)$$

where $$N^T = [n_1, n_2, n_3, n_4] \qquad (2.14)$$

and $$H^T = [-k_0 n_0, 0, 0, 0] \qquad (2.15)$$

(the matrix A is defined overleaf.)

$$A = \begin{bmatrix} -(k_1 + k_{12}a + K_{12}n_0) & (k_{21}a + K_{21}n_0) & 0 & 0 \\ (k_{12}a + K_{12}n_0) & -\{k_2 + (k_{21}+k_{23})a + (K_{21}+K_{12})n_0\} & (k_{32}a + K_{32}n_0) & 0 \\ 0 & (k_{23}a + K_{23}n_0) & -\{k_3 + (k_{32}+k_{34})a + (K_{32}+K_{34})n_0\} & (k_{43}a + K_{43}n_0) \\ 0 & 0 & (k_{34}a + K_{34}n_0) & -(k_4 + k_{43}a + K_{43}n_0) \end{bmatrix} \quad (2.16)$$

Let Δ be the determinant of the matrix A. Then the equation can be solved for N using Cramer's rule. The results are:

$$n_1 = \frac{k_0 n_0}{\Delta} (k_{21} k_{32} k_{43} a^3 + A_1 a^2 + A_2 a + A_3) \tag{2.17}$$

$$n_2 = \frac{k_0 n_0}{\Delta} (k_{12} a + K_{12} n_0)(k_{32} k_{43} a^2 + B_1 a + B_2) \tag{2.18}$$

$$n_3 = \frac{k_0 n_0}{\Delta} (k_{12} a + K_{12} n_0)(k_{23} a + K_{23} n_0)(k_4 + k_{43} a + k_{43} n_0) \tag{2.19}$$

$$n_4 = \frac{k_0 n_0}{\Delta} (k_{12} a + K_{12} n_0)(k_{23} a + K_{23} n_0)(k_{34} a + K_{34} n_0) \tag{2.20}$$

where

$$\begin{aligned} A_1 = {} & \{k_2 k_{32} k_{43} + k_{23}(k_4 k_{34} + k_3 k_{43}) + k_{21}(k_{32} k_4 + k_4 k_{34} + k_8 k_{43})\} \\ & + n_0 \{k_{32} k_{43}(K_{21} + K_{23}) + k_{21}(k_{32} K_{43} + k_{43} K_{32}) - k_{32} K_{23} k_4\} \\ & - k_{32} K_{23} K_{43} n_0^2 \end{aligned} \tag{2.21}$$

$$A_2 = \{k_3 k_4 (k_{21} + k_{23}) + k_2 (k_4 k_{32} + k_4 k_{34} + k_3 k_{43})\}$$

$$+ n_0 \{k_{21} (k_3 K_{43} + k_4 K_{32} + k_4 K_{34}) + k_{23} (k_3 K_{43} + k_4 K_{34})$$

$$+ K_{23} (k_4 k_{34} + k_3 k_{43}) + k_2 (k_{32} K_{43} + k_{43} K_{32}) + K_{21} (k_4 k_{34} + k_3 k_{43})\}$$

$$+ n_0^2 (k_{21} K_{32} K_{43} + k_{32} K_{21} K_{43} + k_{43} K_{21} K_{32}) \qquad (2.22)$$

$$A_3 = k_2 k_3 k_4 + n_0 \{k_2 k_4 (K_{32} + K_{34} + K_{23}) + k_3 (k_2 K_{43} + k_4 K_{21})\}$$

$$+ n_0^2 \{k_2 K_{43} (K_{32} + K_{23}) + k_4 K_{34} (K_{21} + K_{23}) + K_{21} (k_3 K_{43} + k_4 K_{32})\}$$

$$+ K_{21} K_{32} K_{43} n_0^3 \qquad (2.23)$$

$$B_1 = k_4 (k_{32} + k_{34}) + k_3 k_{43} + n_0 (k_{32} K_{43} + k_{43} K_{32}) \qquad (2.24)$$

$$B_2 = k_3 k_4 + n_0 \{k_4 (K_{32} + K_{34}) + k_3 K_{43}\} + K_{32} K_{43} n_0^2 \qquad (2.25)$$

From equations (2.17), (2.18), and (2.19) can be derived:

$$\frac{n_2}{n_3} = \frac{k_{32}k_{43}a^2 + B_1 a + B_2}{(k_{23}a + K_{23}n_0)(k_4 + k_{43}a + K_{43}n_0)} \qquad (2.26)$$

and

$$\frac{n_1}{n_3} = \frac{k_{21}k_{32}k_{43}a^3 + A_1 a^2 + A_2 a + A_3}{(k_{23}a + K_{23}n_0)(k_4 + k_{43}a + K_{43}n_0)(k_{12}a + K_{12}n_0)} \qquad (2.27)$$

If it is now assumed that at the inert gas pressures used, the effects of collisions between caesium atoms is insignificant, these equations become (by putting all K's to zero):

$$\frac{n_2}{n_3} = \frac{k_{32}k_{43}a^2 + B'_1 a + k_3 k_4}{k_{23}a(k_4 + k_{43}a)} \qquad (2.28)$$

and

$$\frac{n_1}{n_3} = \frac{k_{21}k_{32}k_{43}a^3 + A'_1 a^2 + A'_2 a + k_2 k_3 k_4}{k_{12}k_{23}a^2(k_4 + k_{43}a)} \qquad (2.29)$$

where the primes indicate coefficients derived from the corresponding unprimed quantity by making all the K's in the latter equal to zero.

If it is further assumed that inert gas pressure is low enough that transfer of excitation to the $7D_{5/2}$ level is not very probable, then the equations reduce further (by putting rate constants whose subscript is 34 or 43 equal to zero) to:

$$\frac{n_2}{n_3} = \frac{k_{32}}{k_{23}} + \frac{k_3}{k_{23}}\left(\frac{1}{a}\right) \tag{2.30}$$

and

$$\frac{n_1}{n_3} = \frac{k_{21}k_{32}}{k_{12}k_{23}} + \frac{\{k_3(k_{21} + k_{23}) + k_2 k_{32}\}}{k_{12}k_{23}}\left(\frac{1}{a}\right) + \frac{k_2 k_3}{k_{12}k_{23}}\left(\frac{1}{a}\right)^2 \tag{2.31}$$

2.3 INTERPRETATION OF RATE CONSTANTS

(A) Radiative Transitions

k_0 can be evaluated by the equation

$$k_0 = B_{01}\, u(3889) \qquad (2.32)$$

where B_{01} is the Einstein B coefficient for the transition in caesium $6S_{1/2} \rightarrow 8P_{1/2}$ and $u(3889)$ the energy density of radiation at 3889 Å. The latter is difficult to evaluate and, since k_0 does not occur in any of equations (2.26) and (2.27) or their successors, no further discussion of k_0 is necessary.

k_1, k_2, k_3, and k_4 are identical to the reciprocals of the average lifetimes of the states $8P_{1/2}$, $8P_{3/2}$, $7D_{3/2}$, and $7D_{5/2}$ respectively i.e. each k value is equal to the sum of the probabilities (the Einstein A coefficients) of spontaneous transitions from the state concerned to all lower states. The Einstein A coefficients are tabulated (see Appendix I) and so these k-values are known.

(B) Non-Radiative Transitions

The rate constants k_{ij} and K_{ij} for non-radiative transitions are such that $k_{ij}a\ n_i$ and $K_{ij}n_o n_i$ are the rates of collisions between caesium atoms in the relevant excited states (i) with inert gas atoms and caesium atoms in the ground state respectively

which lead to particular different states of excitation (j).

Statistically, the rate of energy transfer in atomic collisions may be represented by a total cross-section Q(T) at temperature T:

$$Q(T) = \int_0^\infty q(E) f_T(E)\, dE \qquad (2.33)$$

where:

E is the relative kinetic energy of colliding atoms,

q(E) is the cross-section for collision between two atoms whose relative kinetic energy lies between E and E + dE,

$f_T(E)\,dE$ is the probability that at temperature T the relative kinetic energy lies between E and E + dE,

$$f_T(E)\,dE = \frac{2\sqrt{E}}{\sqrt{\pi}(kT)^{3/2}} \exp\left(\frac{-E}{kT}\right) dE \qquad (2.34)$$

k is Boltzmann's constant (1.381×10^{-23} J. ^{0}K^{-1})

The rate constant k_{ij} may be similarly expressed

$$k_{ij}(T) = \sqrt{\frac{2}{\mu}} \int_0^\infty q_{ij}(E) \sqrt{E} f_T(E)\, dE \qquad (2.35)$$

That this is so can be more easily seen if it is noted that

$$\sqrt{\left(\frac{2E}{\mu}\right)} = v_r \qquad (2.36)$$

where: μ is the reduced mass of the colliding atoms

v_r is the average relative velocity of colliding atoms and is given by:

$$v_r = \left(\frac{8kT}{\pi\mu}\right)^{\frac{1}{2}} \qquad (2.37)$$

This may be compared with the collision number defined by Seiwert[15].

From equations (2.33) and (2.35):

$$k_{ij}(T) \simeq v_r \int_0^\infty q_{ij}(E) f_T(E)\, dE$$

$$= v_r\, Q_{ij}(T)$$

$$\text{i.e. } Q_{ij}(T) \simeq \frac{k_{ij}(T)}{v_r} \qquad (2.38)$$

So, if the values of k_{ij} can be found, then the total cross-section for the corresponding process can be derived.

2.4 SPECTRAL LINE INTENSITY

The intensity of a spectral line due to a transition from a level α to a level β is $I_{\alpha\beta}$ where:

$I_{\alpha\beta}$ = (Number of transitions/unit time) x Energy of one photon

$$= n_\alpha A_{\alpha\beta} \frac{hc}{\lambda_{\alpha\beta}} \qquad (2.39)$$

in which

n_α = Population density of the level α

$A_{\alpha\beta}$ = Einstein A coefficient for the transition $\alpha \rightarrow \beta$

h = Planck's constant (6.626×10^{-34} J.s)

c = Velocity of light (2.998×10^{8} m.s^{-1})

$\lambda_{\alpha\beta}$ = Wavelength of the spectral line

2.5 DENSITY RATIOS

It is now possible to derive expressions for the density ratios $\frac{n_2}{n_3}$ and $\frac{n_1}{n_3}$ which appear in equations (2.26) and (2.27) respectively.

If the particular radiative transitions from state 2 to state i and from state 3 to state j are considered, then from equation (2.39):

$$I_{2i} = n_2 A_{2i} \frac{hc}{\lambda_{2i}} \qquad (2.40)$$

and

$$I_{3j} = n_3 A_{3j} \frac{hc}{\lambda_{3j}} \qquad (2.41)$$

whence

$$\frac{n_2}{n_3} = \frac{I_{2i}}{I_{3j}} \cdot \frac{A_{3j}}{A_{2i}} \frac{\lambda_{2i}}{\lambda_{3j}} = \frac{I_{2i}}{I_{3j}} \cdot F(_2i, _3j) \qquad (2.42)$$

So the density ratio can be derived from the ratio of the intensities of any two convenient lines emitted from the two states.

2.6 CALCULATION OF CROSS-SECTIONS

The remaining term in equation (2.11) not yet discussed is n_0, the density of ground-state caesium atoms. It is assumed that n_0 is so much larger than the other n_i that it is essentially constant and that, in fact, the partial pressures due to excited caesium atoms are separately and collectively negligible. The value of n_0 is then calculated from the equation

$$p_0 = n_0 kT \qquad (2.43)$$

where p_0 is the vapour pressure of caesium at temperature T in the upper part of the resonance cell (where the reactions occur).

k is Boltzmann's constant.

The quantity a is directly related to the pressure of inert gas by an equation identical in form to equation (2.43):

$$p = a\,kT \qquad (2.44)$$

where p is inert gas pressure

and T is temperature of the upper part of the resonance cell.

In practice then, the intensity ratio is calculated from experimental observations at various

pressure values and the data is fitted to functions of the same form as equations (2.30) and (2.31) modified as shown below.

From equation (2.44):

$$a = \frac{pf}{kT} \tag{2.45}$$

where f is a conversion factor to convert p from torr to $N.m^{-2}$

$$f = 133.3\ N.m^{-2}.torr^{-1}$$

If now equations (2.42) and (2.45) are used, equation (2.30) becomes:

$$R = A + B(1/p) \tag{2.46}$$

where

$$R = \frac{I(8P_{3/2} \rightarrow 5D_{5/2})}{I(7D_{3/2} \rightarrow 6P_{3/2})} = \frac{I(8933\ \text{Å})}{I(6985\ \text{Å})} \tag{2.47}$$

$$A = \frac{k_{32}}{k_{23}F(8933,6985)} \tag{2.48}$$

$$B = \frac{k_3 kT}{k_{23}\ f.F(8933,6985)} \tag{2.49}$$

When B is found, k_{23} can be calculated and then, from A, k_{32} may be evaluated. Hence the cross-sections for the processes $8P_{3/2} \rightleftarrows 7D_{3/2}$ can be derived.

Similarly equation (2.31) becomes:

$$R' = A' + B'(1/p) + C'(1/p)^2 \tag{2.50}$$

where

$$R' = \frac{I(8P_{3/2} \rightarrow 5D_{3/2})}{I(7D_{3/2} \rightarrow 6P_{3/2})} = \frac{I(8921\ \text{Å})}{I(6985\ \text{Å})} \tag{2.51}$$

$$A' = \frac{k_{21} k_{32}}{k_{12} k_{23} F(8921,6985)} \tag{2.52}$$

$$B' = \frac{kT\{k_3 (k_{21} + k_{23}) + k_2 k_{32}\}}{f\, k_{12} k_{23} F(8921,6985)} \tag{2.53}$$

$$C' = \frac{k_2 k_3 (kT)^2}{f^2 k_{12} k_{23} F(8921,6985)} \tag{2.54}$$

Since k_{23} and k_{32} are already known from above, k_{12} may be readily calculated from equation (2.54). Then, using (2.52) or (2.53), k_{21} may be calculated.

3. APPARATUS

3.1 GENERAL

The salient features of the experimental arrangement are shown in Figure 3.1. Caesium vapour (or a caesium vapour-inert gas mixture) in the resonance cell is irradiated with light from the helium lamp. Caesium fluorescence is passed through a chopping wheel, a filter, and a grating monochromator to a photomultiplier. The output from the photomultiplier is amplified by a low-noise amplifier and rectified by a phase-sensitive detector. The reference signal for the phase-sensitive detector is provided by a photodiode whose input is modulated by the chopping wheel and whose output is passed through a phase shifter and amplifier before reaching the phase-sensitive detector. The output of the phase-sensitive detector is fed into a recorder.

3.2 RESONANCE CELL

The resonance cell is constructed from 25 mm pyrex tubing with a right angle bend. It is depicted in Figure 3.2. The pyrex window through which fluorescence is observed has a diameter of 25 mm and is 2 mm thick; it is optically flat with parallel faces. The resonance cell is connected with the ultra-high

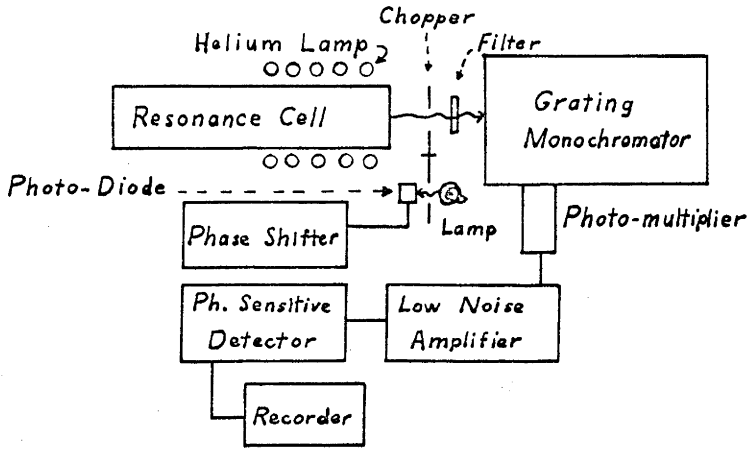

Fig. 3.1 - Experimental Arrangement

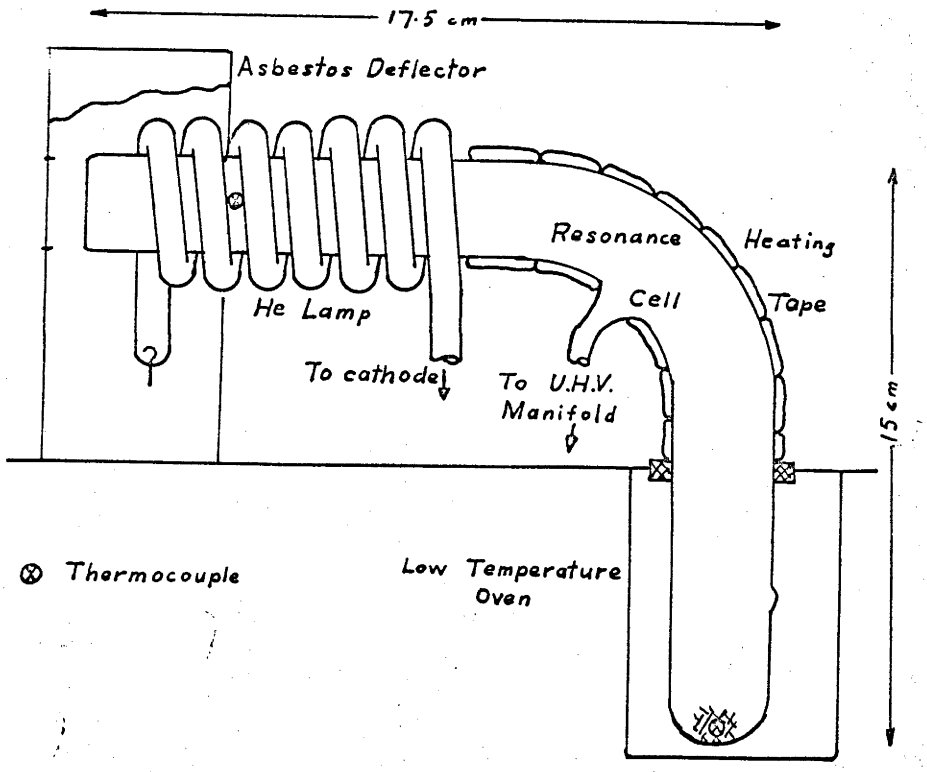

Fig. 3.2 - Resonance Cell

vacuum manifold through a Granville-Phillips Type C ultra-high vacuum valve with a standard manual driver.

The pressure of caesium vapour in the resonance cell is controlled by the lowest temperature in the cell. The upper part of the cell is kept at an elevated temperature (~230°C) by heat dissipated by the helium lamp. Condensation of caesium vapour on the front window is prevented by deflecting some of the heated air around the resonance cell over the window by means of a deflector made of asbestos paper. The temperature of the lower part of the cell controls the pressure and its control is described in section 3.18 below. The measurement of temperature is described in section 3.19.

3.3 HELIUM LAMP

The helium lamp is a conventional direct-current, hollow cathode, glow discharge. It is formed from pyrex tubing of 7 mm internal diameter. As shown in Figure 3.2 it is coupled to the resonance cell by being wound around the upper part of the cell in the form of a helix. The anode is a nickel, hook-shaped wire and the cathode is an open-ended nickel cylinder. The distance between the cathode and the anode in

this arrangement is approximately 130 cm of which approximately 127 cm is positive column. The lamp is connected to the ultra-high vacuum manifold through a Granville-Phillips Type C ultra-high vacuum valve with a standard manual driver.

The lamp is operated at 1.8 torr helium pressure (see section 4.3) and is filled with industrial grade helium. Power to excite the discharge is provided by a Beckman 30 kV, 100 mA Constant Current power supply. It was found that regulation of the output current was not very good at the low (~3 kV) voltage required to operate the discharge tube; presumably the silicon controlled rectifiers which maintain stability of output current were not firing properly at the low voltage. Stable operation of the discharge was achieved by inserting a resistance of 60 kΩ in series with the discharge lamp to increase the output voltage.

3.4 VACUUM SYSTEM

A schematic diagram of the vacuum system is shown in Figure 3.3. The whole system is built in an aluminium frame. The roughing pump is a Rud Browne Dynavac two-stage, air ballast, fractionating, high vacuum pump which provides a backing pressure for the

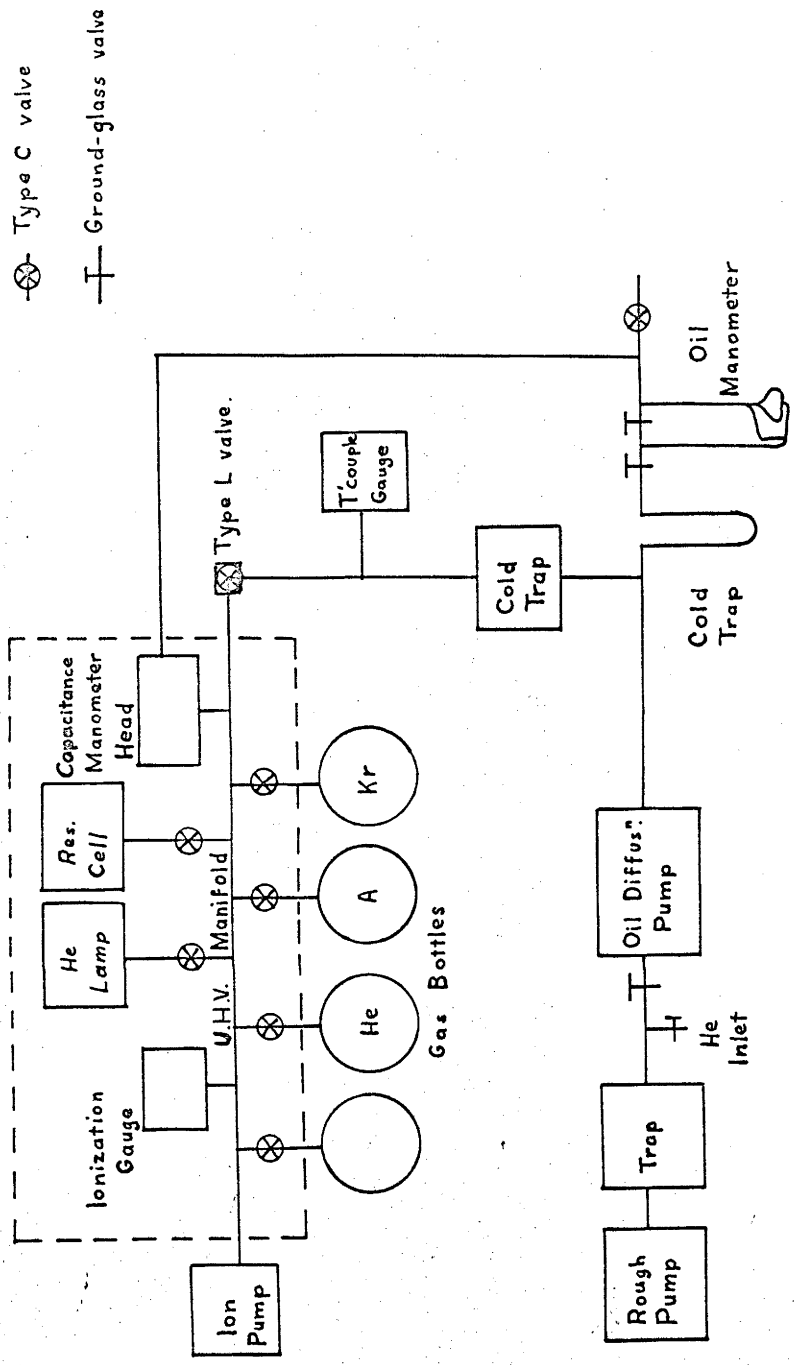

Fig. 3.3 - Vacuum System

fractionating, two-stage, glass, oil diffusion pump. Silicone 704 oil is used in the latter pump. The zeolite trap on the low-pressure side of the oil diffusion pump is immersed in a liquid nitrogen bath. A thermo-couple gauge (Veeco Vacuum Gauge Tube Type DV-1M) which ranges from 1000×10^{-3} to 1×10^{-3} torr is installed on the low-pressure side of the trap.

A Granville-Phillips, one inch, Type L ultra-high vacuum valve with a low-torque driver separates the above-mentioned components from the ultra-high vacuum manifold. The UHV manifold is pumped by an Ultek high-vacuum ion pump which is powered by an Ultek Electronic Pump Power Unit, Model 60-062.

Pressure in the UHV manifold is measured by a Veeco Ionization Gauge Type RG75P and control unit (Veeco Type RG31X) whose range is 10^{-3} torr to 10^{-10} torr. The control unit is also the meter unit for the thermo-couple gauge.

To measure higher pressures in the UHV manifold (for filling the helium lamp and for admitting buffer gases to the resonance cell) a Granville-Phillips Capacitance Manometer (Series 212, Model 03) is attached. The box labelled "Capacitance Manometer Head" in Figure 3.3 actually consists of the sensing

head and balance unit. The latter is removed during bake-out (see section 4.1). The sensing head is not the normal 10 torr head but a 1000 torr head. An oil manometer capable of measuring a pressure difference of about 15 torr is connected to the "dirty" side of the sensing head. The low-pressure side of this is connected through the cold trap to the low-pressure side of the oil diffusion pump. The high-pressure side of the oil manometer is connected to the atmosphere through a Type C Granville-Phillips valve.

Separated from the UHV manifold by Granville-Phillips Type C valves are the helium lamp, the resonance cell, and four gas bottles. Three of the bottles contain respectively helium (Grade X), argon (Grade X) and krypton (99-100% pure, balance xenon), all made by the British Oxygen Company Ltd. These bottles have a breakable glass seal and were sealed on with a "hammer" of glass enclosed steel for breaking the seals later. The fourth bottle is empty to allow use of other buffer gases.

The dotted line on the diagram indicates the section of the system baked out. The oven used was a box made of mild steel sheet. Insulwool was packed

around the outside of the oven and held in place by expanded steel mesh. The heating element consisted of two 1000 W heaters in parallel inside the top of the oven. The oven was placed over the vacuum system covering all the necessary components which were above the asbestos board table top except for the capacitance manometer sensing head which was below the table top. The latter was heated with a heating tape (96 W).

3.5 CAESIUM

The caesium used is obtained from a caesium metal generator manufactured by E.M.I. Electronics Ltd. The generator consists of a nickel container holding a mixture of aluminium, tungsten, and caesium chromate. It is supplied under vacuum in a pyrex glass ampoule. E.M.I. claim that about 0.11 gm of caesium is provided by this. The generator is sealed to the resonance cell during fabrication of the vacuum system and, when required, is further outgassed at 500°C to 600°C using an induction heater.

After outgassing is completed, it is further heated to its firing temperature (about 800°C to 1200°C or higher) when an exothermal reaction takes place in the powder and caesium drifts as liquid and

vapour out of the nickel container and condenses on the walls of the ampoule. It is then forced to drift into the resonance cell by gentle heating with a flame.

Heating is accomplished by use of a Philips 1 kW Inductive Generator Type PH1001/14 which operates at between 1.7 and 2.7 MHz. A copper coil of two turns attached to the output terminals is placed so that the ampoule lies at its centre.

3.6 CHOPPING WHEEL

The chopping wheel is an aluminium disc with six holes around the outer edge so positioned and of such size as to give equal times for "on" and "off". The holes have radii of the disc for two sides and concentric circles form the other two "sides".

A 240V domestic fan motor turns the wheel at a speed such that the chopping frequency is 142 Hz. The whole arrangement (motor and disc) is mounted on the monochromator in front of the input lens.

3.7 GRANVILLE-PHILLIPS VALVES

These are metal valves designed for ultra-high vacuum. Their main features are low vapour pressure materials in regions which come into contact with the vacuum and ability to be baked if certain pre-

cautions (section 4.1) are taken. Closing of the valve is achieved by screwing a bolt which presses a nosepiece of monel metal which a silver gasket into a hole which is then sealed. The nosepiece is held by a nickel diaphragm which allows it to move in and out. Careful adjustment can allow the valve to be opened very slightly so that a slow leak of gas through it is possible.

3.8 FILTER

As shown in Figure 3.1 a filter is used through which the fluorescent light passes before entering the monochromator. A Kodak Wratten filter, No. 8 was used. This filter transmits all wave-lengths greater than 4600 Å. At 8900 Å its transmission is greater than 90%. The filter consists of a gelatine filter cemented between two optical glass flats.

3.9 MONOCHROMATOR

The monochromator used is a Bausch and Lomb 500 mm grating monochromator (Serial No. GD 33). The optical arrangement is a modified Ebert spectrograph[10] with the mirror and grating at an angle of about 30^{o} to the plane of the slits.

As indicated in Figure 3.4, light from an illuminated slit is directed to a concave collimating-

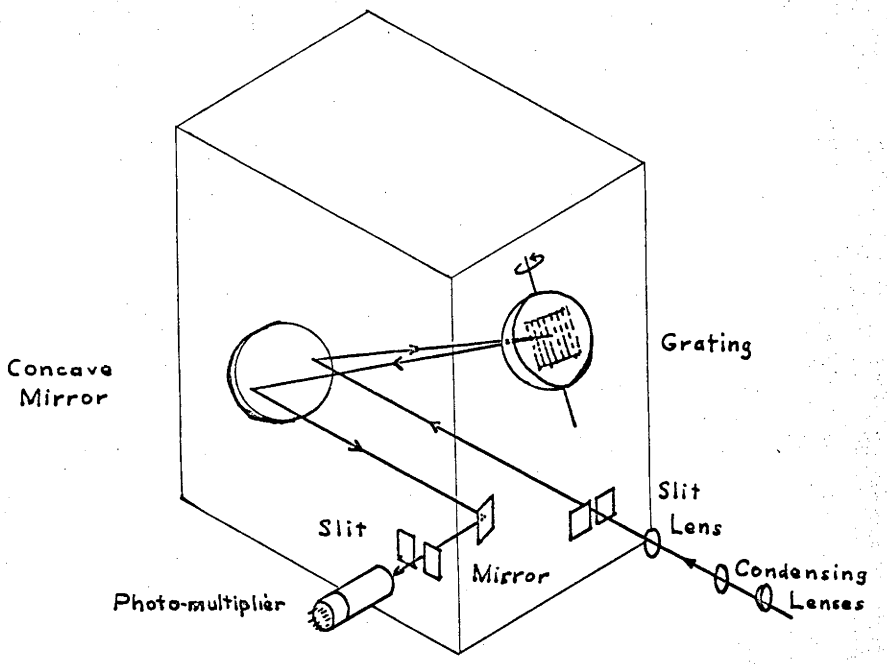

Fig. 3.4 - Monochromator Optics

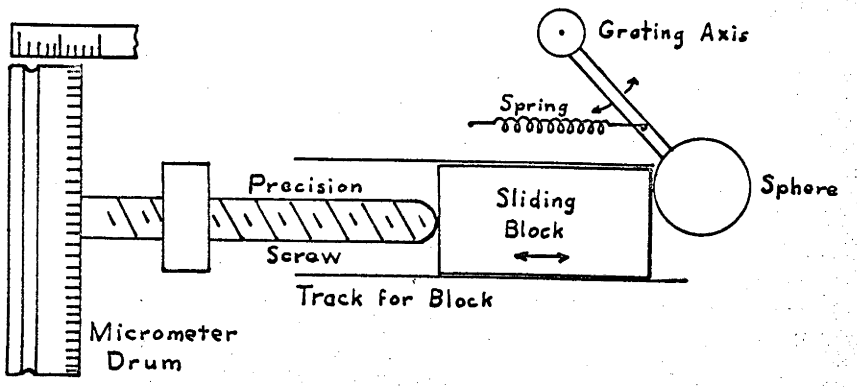

Fig. 3.5 - Sine-Bar Mechanism

condensing mirror, dispersed by a plane grating and reflected back to the same mirror followed by a small plane mirror which reflects it onto the exit slit beyond which lies the photo-multiplier tube. Both slits lie in the focal plane of the concave mirror and so the beam is collimated by the mirror for all wavelengths. Since it acts in a dual capacity, the mirror is larger than the parallel beam so that full aperture is obtained in both the entering and dispersed beams. The equivalent aperture ratio is f4.4.

Both slits are bilateral, symmetrically-opening and identical. The jaws are operated in opposition by a double screw mechanism actuated by a micrometer drum divided into hundredths each complete turn being one millimetre which is indicated by a scale above the drum. The slits open to 12 mm and have a variable height from 0 mm to 20 mm controlled by a V-slide calibrated in 5 mm steps.

The grating rotates to place different wavelengths on the exit slit. The rotation is controlled by a screw contacting a sine bar linkage. This allows a strictly linear wavelength scale to be inscribed on the micrometer drum attached to the outer end of the

screw as shown in Figure 3.5. A groove in the micrometer drum allows the monochromator to be driven for scanning purposes. A small electric-clock motor drives the drum via a gear box, pulley, and rubber "O" ring.

3.10 DIFFRACTION GRATING

The grating used in the monochromator is a Bausch & Lomb "Certified Precision" diffraction grating (catalogue no. 33-53-16-03). It is a plane grating ruled on a circular glass blank 160 mm in diameter and 20 mm thick. The ruled area is 102 mm x 102 mm. There are 1200 grooves per millimetre; dispersion is 16.5 Å/mm (first order) and the grating is blazed for 3000 Å in the first order.

The instrument efficiency for the monochromator with this grating as supplied by Bausch & Lomb is given in Table 3.1. (See over page and also section 4.4).

3.11 PHOTOMULTIPLIER

An E.M.I. Type 9684A photomultiplier was used. The tube has a flat faced end window with a 44 mm diameter semi-transparent cathode and eleven venetian blind type dynodes.

The photo-cathode is an S-1 type whose spectral

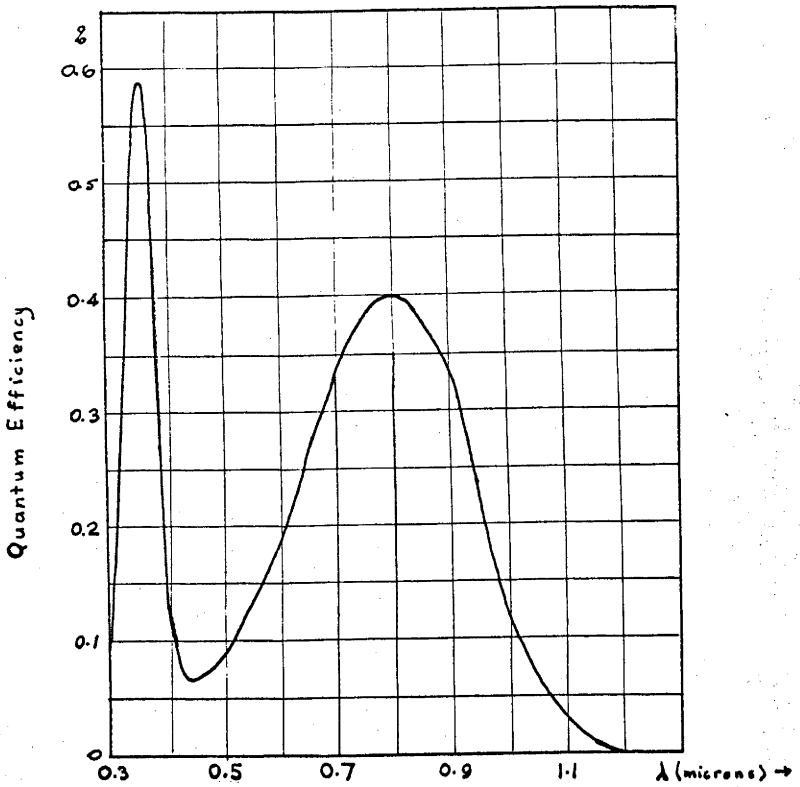

Fig. 3.6 - S-1 Spectral Sensitivity (23)

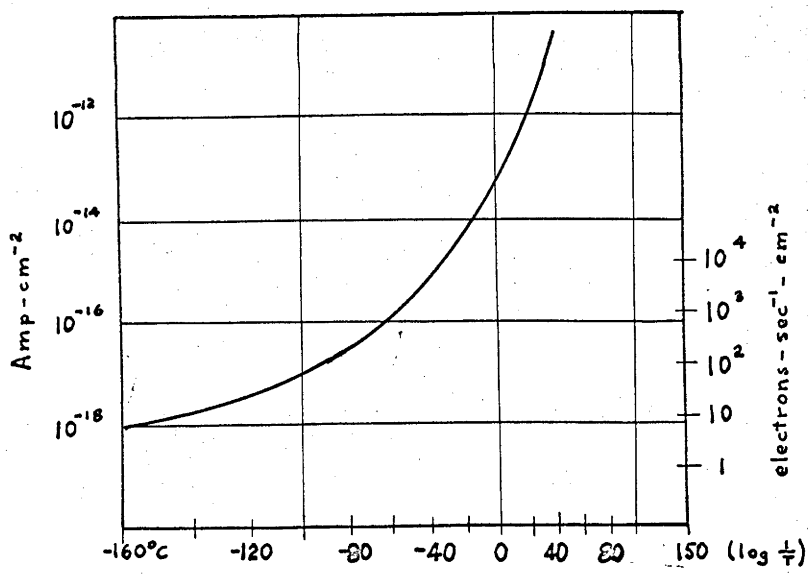

Fig. 3.7 - Cathode Dark Current Variation (23)

WAVELENGTH (Å)	EFFICIENCY (%)
2310	29
2540	36
3100	38
3650	32
4040	30
4350	28
5460	23
5780	15

Table 3.1 - Monochromator Efficiency

sensitivity is shown in Figure 3.6. This type of photo-cathode (composition Ag O Cs) is the only one known with any sensitivity in the proximity of 8900 Å; the quantum efficiency is low, however, being only 0.4% at 8000 Å as shown in figure 3.8 taken from the manufacturers specifications. (There are better photomultipliers in existence, for example Philips 56CVP, but the one used was the only one readily available.) Because of its sensitivity in the near infra-red, the photocathode has a comparatively high dark current which diminishes by several orders of

magnitude if cooled to dry ice temperature. The variation of cathode dark current with temperature is shown in Figure 3.7 taken from the manufacturer's specifications. With the cooling arrangement used, the anode dark current was 5.5×10^{-12} A after cooling for one hour.

The venetian blind dynode arrangement is stated by the manufacturers to give the best gain stability with time of all dynode configurations.

The dynode resistance chain is the type described by the manufacturers as "linear" simple high gain and is shown in Figure 3.8. The Zener diodes provide a stabilized voltage K-D1 to minimize variation of gain. The capacitors C are decoupling capacitors; the 0.25μF capacitor is to prevent large pulses passing which may damage the detector circuitry.

The power supply for the photomultiplier is a John Fluke Model 405L DC Power Supply whose stability is stated as 0.005% per hour, 0.05% per day and whose ripple and jitter is stated to be less than 5 mV r.m.s. at any output voltage and current.

Table 3.2 shows the variation of temperature at the photo-cathode and anode dark current with time after commencement of cooling. The former was meas-

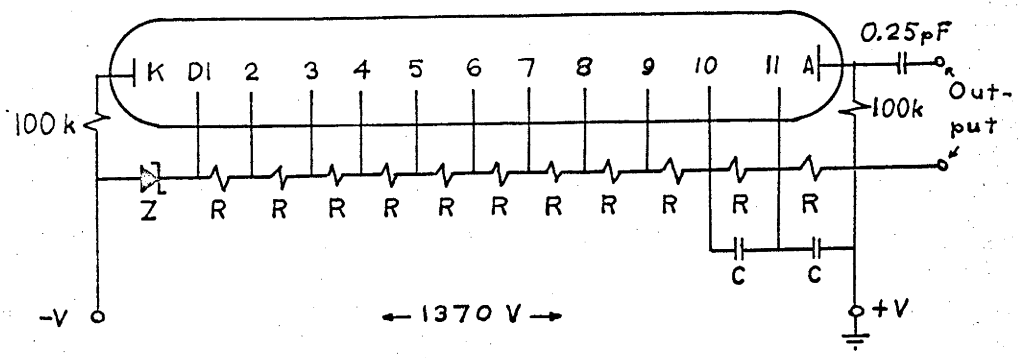

Z = 2 x 75 V Zener Diodes R = 27 kΩ C = 0.47 μF

K = Cathode D = Dynode A = Anode

Fig. 3.8 - Photomultiplier Dynode Chain

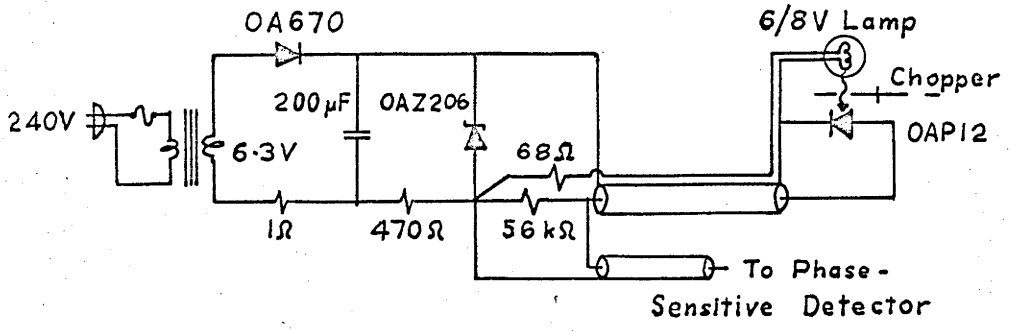

Fig. 3.9 - Circuit for Reference Signal for Phase-Sensitive Detector

ured using a copper-constantan thermocouple inserted next to the photo-cathode while the latter was measured with a General Radio DC Amplifier and Electrometer. The heating coil which was originally switched off was turned on after 65 minutes.

Cooling Time (minutes)	Photo-cathode Temperature (^{o}C)	Anode Dark Current (A)
0	30 (Ambient)	-
5	23	6×10^{-7}
10	0	9×10^{-8}
15	-25	3.5×10^{-8}
20	-37	1.8×10^{-8}
25	-51	6.4×10^{-9}
30	-60	1.6×10^{-9}
35	-66	5.8×10^{-10}
40	-71	1.7×10^{-10}
45	-76	5.3×10^{-11}
50	-79	1.9×10^{-11}
55	-81	8.5×10^{-12}
60	-84	7.0×10^{-12}
65	-86	5.5×10^{-12}
(Switch on heating coil)		
70	-83	5.0×10^{-12}
75	-81	5.0×10^{-12}
80	-80	3.7×10^{-12}
85	-79	3.6×10^{-12}
90	-79	3.3×10^{-12}
95	-78	3.4×10^{-12}

Table 3.2 - Photomultiplier Dark Current

In connection with table 3.2, it is notable that after the heating coil was switched on the thermocouple indicated a slight rise in temperature but the dark current continued to fall slightly. This would be due to the thermocouple's being closer to the heater than the photo-cathode is and, also, as shown in Figure 3.10, to the nylatron insulation between the heater and the photo-cathode. It should also be noted that, in actual use, a higher heating current was used so that the dark current was about 10^{-10} A.

3.12 PHOTOMULTIPLIER HOUSING

The housing is made of brass and, as shown in Figure 3.10, consists basically of a cylinder approximately 3½" in diameter and 11" long with screw-on ends. The front end-piece has a 30 mm polished silica window set into it which is held in place by a nylon collar and a brass screw-in ring. On the outside of the front end-piece is a male screw thread which screws into the monochromator at the exit slit. Rubber seals are provided at all the joints to keep the housing moisture-proof and silica-gel is placed inside the housing to keep the interior dry.

Provision is made for a heating coil to be

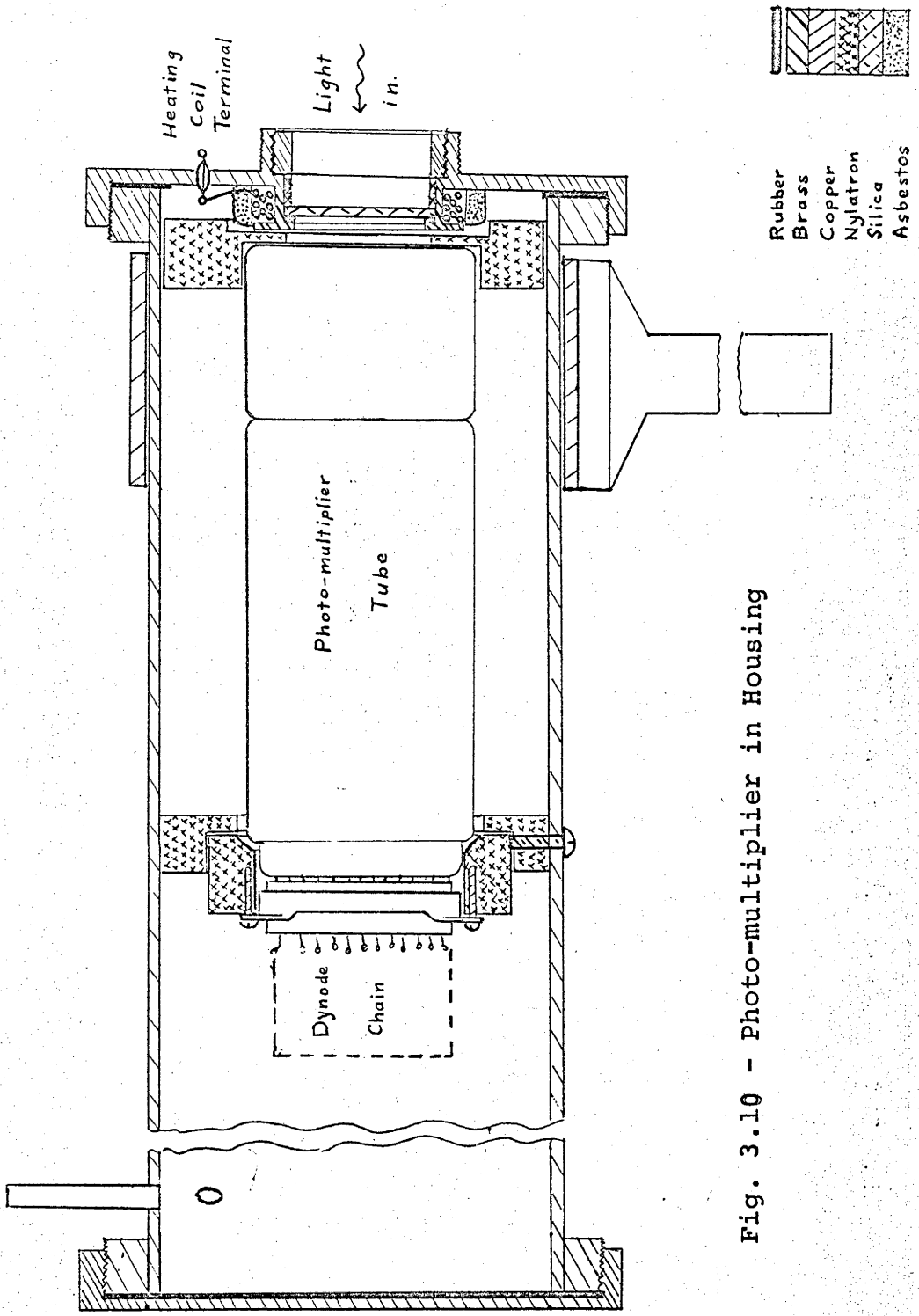

Fig. 3.10 - Photo-multiplier in Housing

positioned around the circumference of the glass window to reduce frosting on the window. The coil is wound with Eureka wire (24SWG) which is enamelled and silk covered. The coil resistance is 11 Ω. Two glass lead-throughs are inserted in the front end-piece for the electricity supply to the heating coil. The heating coil is covered on its outer circumference by asbestos to keep heating of the photocathode to a minimum. Operation of the coil is from the mains through a Variac auto-transformer and a 240V-32V step-down transformer set so that about 16V is supplied to it.

The photomultiplier is supported by a nylatron ring so that the photo-cathode is just inside the silica window. The teflon base of the photomultiplier is similarly supported by a nylatron ring. The dynode resistor chain is built on the underside of the base. Power to the photomultiplier and signals from it are carried by doubly shielded co-axial cables which enter and leave the housing through two two-inch brass tubes welded radially to the cylinder axis. This arrangement keeps the cables relatively firmly in place.

Cooling of the photomultiplier is achieved by

a copper band three inches wide wrapped around the cathode end of the housing. Brazed to the two ends of the band are two copper rods one inch wide and one-quarter inch thick which are clamped together and immersed in a dewar of liquid nitrogen. The whole housing is insulated by expanded polyurethane foam about one inch thick. With this arrangement it is possible to obtain a temperature of about $-80^{\circ}C$ after one hour of cooling.

The housing is over-sized for the photomultiplier that it contains. This is because it was designed originally for a Philips 56 CVP photomultiplier which had been ordered for the experiment. When the Philips tube failed to arrive, the EMI tube which is physically smaller was substituted.

3.13 PHASE-SENSITIVE DETECTOR REFERENCE SIGNAL

This basically consists of a 6V lamp and OAP 12 photo-diode for which a rectifier provides power and bias voltage respectively. The output signal is the voltage across a 56 kΩ load resistor. The circuit is shown in Figure 3.9.

The lamp and diode are mounted on opposite sides of the chopper at about 180° with respect to the in-

put lens of the monochromator.

3.14 LOW-NOISE AMPLIFIER

The signal from the photomultiplier is pre-amplified by a Brookdeal Model LA350 Low-Noise Amplifier. This has a maximum gain of 100 db and the output can be attenuated from 0 to -55 db in 5 db steps. The attenuators are distributed feedback attenuators and act by changing the closed loop gain so that any noise is attenuated by the same factor as the signal.

The upper and lower 3 db points are adjustable and were set for this experiment at 300 and 100 Hz respectively. The high and low pass filters in the amplifier allow bandwidth reduction while introducing negligible phase shift at the centre of the pass-band, an important advantage in phase-sensitive detection.

The noise figure for a source resistance of 100 kΩ at 142 Hz is about 1 db when using the high-Z input.

3.15 PHASE SHIFTER

This unit is actually a Brookdeal Model PP313A Phase-Sensitive Detector/Phase Shifter of which only

the phase shifter part is used. This is necessary to adjust the phase of the reference signal with respect to the signal and also because the phase shifter contains an amplifier to amplify the signal to the level (>3 V peak-to-peak) required for the reference input of the phase-sensitive detector. The frequency range is selectable and is set for this experiment in the range 100 - 300 Hz.

An R-C phase shifting network is employed in this device. The resistance R is a 10 kΩ logarithmic potentiometer and adjusts the phase. Different values of C are switched in for different frequency ranges.

3.16 PHASE-SENSITIVE DETECTOR

A Brookdeal Model PM 322 Phase-Sensitive Detector/Meter Unit is used. Features include high linearity and low zero drift (< 0.01% per ^{o}C). There is an output meter and output terminals suitable for a pen recorder (± 10 mV out of 800 Ω). The frequency range is 3 Hz to 300 kHz.

Output controls include a time constant switch (0, 0.03, 0.1, 0.3, 1, and 3 sec, and external), a filter for removing low frequency flicker, an attenuator (0, -10, -20 db), and a zero-suppression control.

All of the Brookdeal equipment used have "Mains Earth" switches through which the chassis are connected to the mains earth leads. The switch is a three way switch allowing direct connection to earth, indirect connection (via 47 Ω), or disconnection. This switch enables earth loops in multi-instrument systems to be eliminated. In this experiment all the mains-earth switches were set at "Disconnect" and earthing was via input and output leads.

3.17 T-Y RECORDER

A Houston Instrument Corporation T-Y Recorder (Model HR-87) was connected across the recorder-output terminals of the phase-sensitive detector. The unit is a servo-driven graphing device which plots voltage along the Y-axis (11" long, maximum sensitivity 1mV/in) against time along the T-axis (17" long). Three plug-in scanning motors permit traverse times of 24 hr, 1 hr, and 6 min. The input resistance is 10 kΩ and output is plotted on graph paper 10" x 15". Maximum vertical pen speed is 7½" per second.

An isolation transformer was used to provide power so that the recorder was floating. The re-

corder was used to scan regions of the spectrum in conjunction with the scanning motor on the monochromator. In this respect the set-up left much to be desired due to the lack of direct connection between the two mechanisms. The difficulty in starting the T-axis drive at a precise instant and the inconstant driving of the monochromator by the rubber "O" ring (due to slipping and stretching) made accurate scanning impossible. A suitable arrangement would have been an X-Y recorder whose X-axis is controlled by a potentiometer attached to the micrometer drum of the monochromator.

3.18 CAESIUM VAPOUR PRESSURE CONTROL

As mentioned in section 3.2, the vapour pressure of caesium in the resonance cell is controlled by the lowest temperature in the cell. This is arranged to be in the lower part of the cell (see Figure 3.2).

A small steel tube with a bottom welded on is covered with asbestos paper on which is wound a Nichrome heating coil (resistance 50 Ω) which is covered externally by asbestos paper. The heating coil is supplied from the mains through a Variac autotransformer.

The vapour pressure of caesium is then calculated from the equations determined by Taylor and Langmuir[11]. These are:

(a) for solid caesium ($T<302^{o}K$)

$$\log_{10} p_s = 10.5460 - 1.00 \log_{10} T - 4150/T$$

and (b) for liquid caesium ($T>302^{o}K$)

$$\log_{10} p_L = 11.0531 - 1.35 \log_{10} T - 4041/T$$

In both cases, T is the absolute temperature in ^{o}K and p is the vapour pressure in torr. Taylor and Langmuir state that these equations are believed to be accurate to within one percent from 220^{o} to $350^{o}K$ and to within three percent up to $600^{o}K$.

If T is the temperature in the upper part of the resonance cell and T' the temperature in the lower portion controlling the vapour pressure p', then the pressure of caesium vapour in the upper part (p) is given by,[12]

$$p = p' \sqrt{\left(\frac{T}{T'}\right)}$$

3.19 TEMPERATURE MEASUREMENT

Temperatures are measured in the upper and lower portions of the resonance cell by means of two Chromel-Alumel thermocouples. They are positioned as indicated in Figure 3.2, the upper one being placed against the wall of the cell. The outer side of the lower thermo-

couple is covered by asbestos so that it reads the temperature of the resonance cell only.

Temperatures are read directly in degrees Centigrade from a Cambridge meter.

3.20 X-Y RECORDER

Late in the project there became available a Plotamatic 810A X-Y Recorder manufactured by Bolt, Beranek and Newman Inc. With this device it was possible to plot intensity of each spectral line against temperature in the case of caesium-caesium collision experiments and against inert gas pressure in the case of caesium-inert gas collisions. Actually, in the former case the e.m.f. produced by a chromel-alumel thermocouple was plotted along the X axis. Inert gas pressure was plotted by using the recorder output terminals of the capacitance manometer.

The recorder has two, identical, independent, self-balancing servo-systems which control the X and Y axes in accordance with separate input signal variations. The voltage ranges on each input are 0.5, 1, 2, 5, 10, 20, 50, and 100 mV/in and 0.2, 0.5, 1, 2, 5, 10, 20 and 50 V/in with a vernier adjustment that allows for settings between the fixed

steps. Input impedance is 1MΩ on all ranges but essentially infinite at null when in the potentiometric mode. Source impedance must be less than 20 kΩ. Accuracy is specified as ± 0.15% of full scale on both axes. Maximum slewing speed is 16.7 in/sec. The recorder plots on 11 x 17 in. paper having a recording area of 10 x 15 in.

4. EXPERIMENTAL PROCEDURE

4.1 ACHIEVEMENT OF VACUUM

Pumping was initiated by use of the rotary roughing pump which, in a matter of minutes, brought the pressure down to about 10^{-3} torr. This pressure was sufficiently low to enable the oil diffusion pump to be switched on.

Before switching on the oil diffusion pump, the dewar in which the cold trap was immersed was filled with liquid nitrogen. This prevented back-streaming of pump oil or thermal decomposition products of the oil into the high vacuum region of the system. The oil diffusion pump was able to reduce the pressure to about 10^{-6} torr in approximately fifteen minutes.

At this stage the isolation valve (Granville-Phillips Type L) was closed with a torque wrench to a torque of 10 ft.lb and the ion pump started. The oil diffusion pump was then able to be switched off.

Next, the driving mechanisms of all the Granville-Phillips Type C valves connected to the UHV manifold were removed and bake-out clamps attached. The clamps kept the gaskets apart from the valve

seats during bake-out thus eliminating the possibility of the components' being welded together.

The balance unit of the capacitance manometer contains electronic components which are not bakeable so this was detached from the sensing head. Since the sensing head is below the table-top, and hence not inside the oven, it and the glass tubing leading to it from the UHV manifold were wrapped with a heating tape.

The oven was lowered over the table-top and switched on together with the heating tape. Bake-out was carried out for 50 hours and the maximum temperature reached (determined by a chromel-alumel thermocouple placed at about the centre of the table-top) was 238^{o}C.

One day after the oven was switched off and the system allowed to cool down, the ion pump having run continuously, the pressure was 3×10^{-9} torr. During this period, the ionization gauge was degassed by turning on the inbuilt heating coil. This causes the heating coil itself to outgas first and, slightly later, the inner glass walls outgas through being heated by radiation. Also, the caesium capsule was outgassed by heating for about a

quarter of an hour with the r-f induction heater. About a day later, the pressure was 1.5×10^{-9} torr.

A procedure similar to the one described above was followed several times for de-bugging to be carried out. One aspect of the de-bugging was leak-testing of the vacuum system. Pin-hole leaks in the glass can be detected in the normal way by using a Tesla coil whose output is led to an explorer electrode. This method is applicable at pressures of the order of one torr. The method can not be used in proximity to metal parts.

At lower pressures the ionization gauge can be used to test for leaks in conjunction with acetone or some other volatile liquid. When acetone is sprayed on a leak one of two things may happen:- (a) the ionization gauge will show an increase in pressure or (b) the ionization gauge will show a decrease in pressure. By spraying small areas of surface, it is therefore possible to detect a leak.

The best method of repairing a leak is to re-make the part concerned. Leaks in the rough vacuum section of the system can be plugged with Glyptal, an alkyd resin with low vapour pressure.

For ultra-high vacuum, however, an epoxy resin such as "Torr Seal" (made by Varian Associates, Vacuum Products Division) which has a very low vapour pressure is better. "Torr Seal" is recommended for small leaks for pressures to 10^{-8} torr and lower, for larger leaks to 10^{-7} torr.

4.2 RELEASE OF CAESIUM

The caesium ampoule was described earlier in section 3.5. The ampoule was attached to the UHV system in such an attitude that the r-f generator could be wheeled into position, the two-turn coupling coil just surrounding the ampoule. The generator was switched on at an out-put power (~100W) sufficient to cause the nickel container to heat to about 500°C to 600°C at which temperature it glowed dull red. This procedure continued for about three hours until most of the gas had been liberated, at which stage the background pressure was ~10^{-8} torr.

After out-gassing to this stage, the output power of the induction heater was stepped up to 250 W until the nickel container reached its firing temperature when caesium metal drifted out of the container and condensed on the inner walls of the ampoule. The caesium was then forced along the connecting

tube from the ampoule to the resonance cell by gentle heating with a flame. The ampoule and connecting tube were then removed. The caesium was kept in the resonance cell by heating the tube joining the cell to the Granville-Phillips valve with a heating tape.

4.3 HELIUM LAMP

To fill the helium lamp, all valves leading off the UHV manifold except that one leading to the helium lamp were closed. Helium pressure was measured by the capacitance manometer used as a null indicator. To do this, the pressure on both sides of the diaphragm is made as (equally) low as possible by pumping with the oil diffusion pump and the capacitance manometer zeroed on all three ranges. Next the oil manometer was closed off from the pump, the valve connecting both sides of the manometer was closed, and air was allowed to leak in through the Granville-Phillips Type C valve until the height of the oil column was equivalent to 1.8 torr pressure (S.G. of manometer oil = 0.866).

Industrial grade helium was allowed to leak into the system through the glass valve (the oil diffusion pump being still on) and pumped out again four or five times to "flush out" the system. The

helium passed through the cold trap filled with liquid nitrogen which would help keep out some impurities. It is expected that the helium was further purified by the process of gas cataphoresis. On the final pump-out the Type L isolating valve was almost closed so that the helium was only slowly pumped out. When the capacitance manometer gauge read zero (≡1.8 torr) the isolating valve was closed. Then the Type C valve connecting the UHV manifold with the helium lamp was closed to a torque of 35 ft.lb. The isolating valve was opened and the UHV manifold pumped out, first by the oil diffusion pump to ~10^{-6} torr and then, after closing the isolating valve (10 ft. lb torque), by the ion pump. The pressure in the helium lamp immediately before admission of helium was ~10^{-6} torr.

The pressure for optimum light power out-put was determined in the following manner: A laser power monitor (Scientifica & Cook) detector was placed end-on to the resonance cell and kept in that position. The helium lamp was then filled at different pressures ranging from 0.5 torr to 7.4 torr. (Pressure was determined from the capacitance manometer which had been calibrated to read pressure

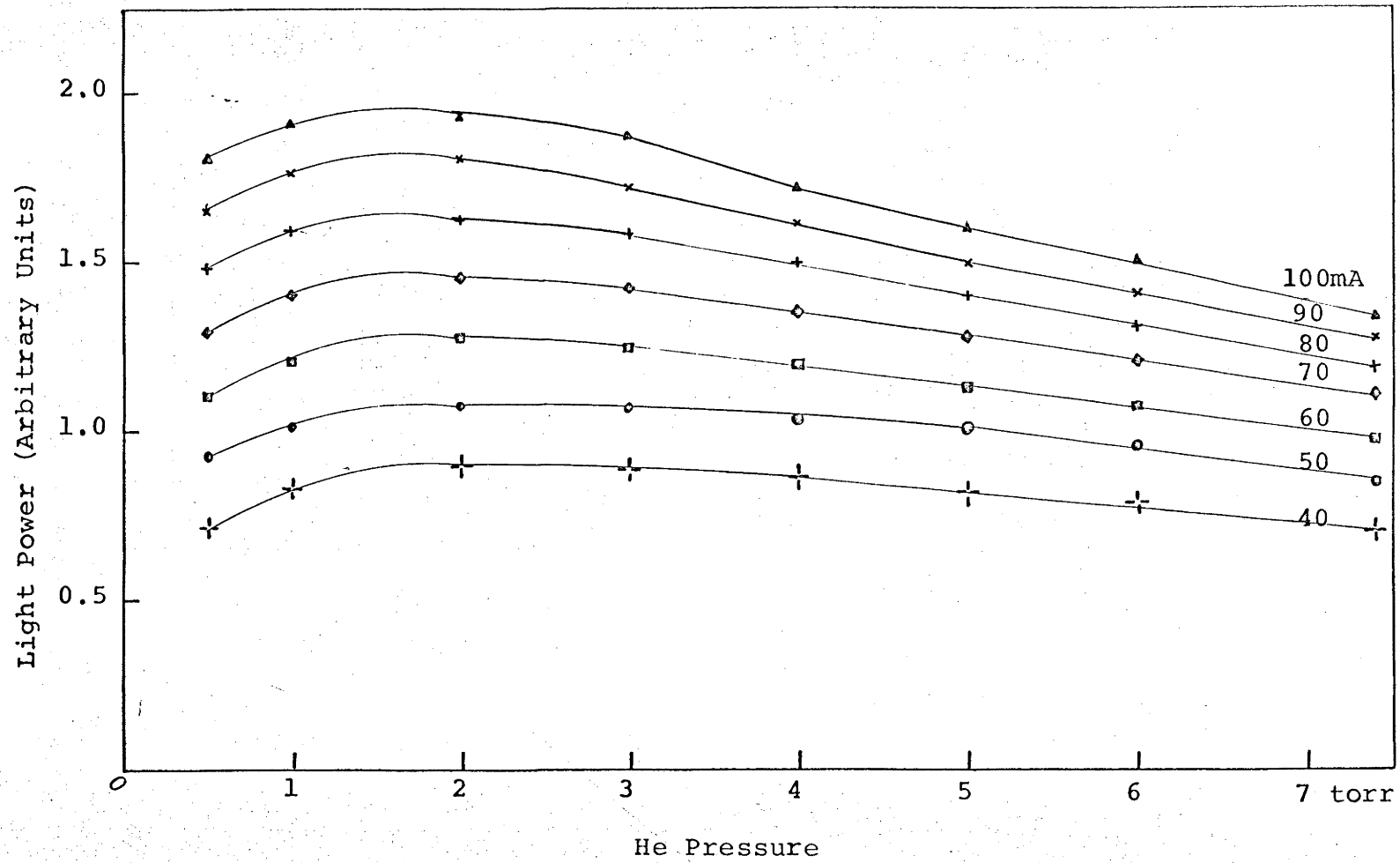

Fig. 4.1 - He Lamp Characteristics

directly in the range 0 to 10 torr.) At each pressure, the discharge was run at various values of discharge current and the reading on the light power meter recorded. (See Figure 4.1.) Finally, the pressure was set at the high end of this range, the discharge initiated, and the isolating valve of the UHV manifold opened slightly so that the pressure slowly reduced (being pumped by the oil diffusion pump). The pressure at which the laser power monitor gave the highest reading was 1.8 torr.

4.4 CALIBRATION OF SPECTROPHOTOMETER

The monochromator was lined up by eye before attaching the photomultiplier housing at the exit slit. With the helium lamp on, the monochromator was set on one of the visible helium lines and the alignment adjusted so that the line of sight was as close as possible to along the axis of the resonance cell. The slits were then closed down so that almost none of the helium lamp coils could be directly seen. The width of the slits was then 0.55 mm and the height about 1 mm. This alignment was not disturbed throughout the experiment. A considerable amount of black cloth was used to

cover the monochromator since it had been discovered previously that light leaking into the monochromator, particularly where the exit slit adjustments are made, was swamping the signal.

In order that the intensities of light at 6985 Å ($7D_{3/2} \rightarrow 6P_{3/2}$) and 8921 Å ($8P_{1/2} \rightarrow 5D_{3/2}$) could be compared, it was necessary to calibrate the spectrophotometer to the extent that the relative efficiencies at these wavelengths was known. (The efficiency at 8933 Å ($8P_{3/2} \rightarrow 5D_{5/2}$) was not discernibly different from that at 8921 Å.)

A tungsten filament lamp was arranged to shine on the entrance slit of the spectrophotometer and the relative output signals at the recorder for settings of 8921 Å and 8933 Å were obtained. The colour temperature of the filament which was powered by a constant current source set at 9A was measured by means of an optical pyrometer and found to be 1450°C. Using Planck's radiation law and emissivity tables for tungsten[16] to correct it, the relative efficiency was found to be given by:

$$\frac{\eta(8921\ \text{Å})}{\eta(6985\ \text{Å})} = 0.2180$$

where $\eta(\lambda)$ is the efficiency at wavelength λ.

4.5 CALIBRATION OF ATTENUATORS

Attenuation adjustments were available on both the low-noise amplifier and the phase-sensitive detector. The former was nominally adjustable in 5 db steps from 0 db to -55 db; the latter consisted of two push-buttons each providing attenuation of -10 db.

The system was checked by using a Hewlett-Packard 205AG Audio Signal Generator to provide a reference signal for the phase-sensitive detector and also, through an attenuator, the input signal to the low-noise amplifier. The attenuator used was a Marconi TF 2162 M.F. Attenuator which has a range of 0 to 111 db in 0.1 db steps. Its accuracy is specified as ±1% of db setting ±0.01 db.

The system was switched on and a signal giving a known output as read on the meter of the phase-sensitive detector was applied. The attenuation control on the low-noise amplifier was altered by 5 db and the Marconi attenuator adjusted to compensate. The change in the Marconi attenuator was taken to be the true attenuation. A similar test was carried out for each of the attenuation adjustments on the phase-sensitive detector.

The results obtained were:

Nominal Attenuation	True Attenuation
(a) Low noise amplifier	
0 db	0 db
5 db	4.7±0.05 db
10 db	9.8±0.1 db
15 db	14.9±0.15 db
(b) Phase sensitive detector	
0 db	0 db
10 db	10.2±0.05 db (both buttons)

4.6 OPERATION OF APPARATUS

Where possible, electronic apparatus such as the capacitance manometer power unit and the Beckman and the Fluke power supplies were left on to reduce the effects of warming-up on the experiment. In the case of the latter power supplies the output voltage was switched off except when in use.

The apparatus was turned on at least one hour before the actual experiment was carried out to enable it to stabilize to some degree. Starting the apparatus involved the following procedure:

(a) The helium lamp usually required to be refilled before each experimental run. This pro-

cedure is described in section 4.3. The lamp invariably required assistance to start. Two Tesla electrodes were used for this purpose, one to start the discharge and the other to guide it to the nickel cathode rather than to the Granville-Phillips valve which seemed to be preferred as a cathode by the discharge.

(b) The low temperature oven may have been switched on at this stage depending on the requirements of the particular experiment.

(c) A hot-air blower was switched on and directed onto the front window of the resonance cell to prevent condensation of caesium there. This device works by blowing air over a heating coil and was, during one of the experimental runs, found to be the source of some hitherto ineradicable noise in the detection system. A simple adjustment of the asbestos-paper deflector was then found to heat the front window sufficiently so the hot-air blower was dispensed with in later experimental runs.

(d) The liquid nitrogen dewar was filled to cool the photomultiplier whose power supply was then turned on as was the heating coil for the entrance window. When the experimental runs were be-

ing carried out, the dewar was topped up with liquid nitrogen at frequent intervals.

(e) The rest of the detection apparatus was then switched on i.e. low-noise amplifier, phase-shifter, phase-sensitive detector, reference signal, chopper wheel, and recorder.

After experiments in which an inert gas was admitted to the resonance cell the gas had to be removed. To do this, the low temperature oven was removed and a small container of liquid nitrogen substituted to condense the caesium in the lower half of the resonance cell. (A plastic-coated, cardboard, hot-drink cup was found to be an ideal container for this purpose.) The condensation was fairly rapid. This was observed on one occasion when fluorescent radiation was being observed at the time that liquid nitrogen was placed in position. The intensity of fluorescence dropped almost immediately and rapidly. (It is probably reasonable to assume from this that mixing of caesium vapour and inert gas when the latter was leaked in was also a rapid process.) When the caesium was condensed, the resonance cell was opened to the oil-diffusion pump

at first and then to the ion pump. The valve was then closed and the liquid nitrogen removed. After a period the process was repeated several times over a period of about a day. By this means it was possible to reduce the pressure in the resonance cell (with liquid nitrogen in place) to less than 10^{-6} torr.

The details of operation of the apparatus for specific experiments are described below.

4.7 SCANNING THE FLUORESCENT SPECTRUM

This experiment was carried out for a particular fixed temperature of lower oven and fixed inert gas pressure. The slowest scanning motor was used on the monochromator which scanned 50 Å in one minute. This speed was too fast to allow the detection system to separate the 8933 Å line from the lines on either side (8946 Å and 8921 Å) since the time constant used at the output of the phase sensitive detector was 3 sec. The output was recorded with the T-Y recorder. Although this has disadvantages (see section 3.17), these were not important for this experiment.

The fluorescent spectrum was scanned from 9000 Å (the highest wavelength possible with the monochro-

mator) to 4600 Å, the lower limit being set by the filter used. The one-hour traverse motor was used on the T-Y recorder for recording purposes. Scans of the region of the spectrum from 9000 Å to 8600 Å using the 5 minute traverse motor showed that the inability to separate out the 8933 Å line was due to the scanning motor driving the wavelength drum of the monochromator.

4.8 CAESIUM-CAESIUM COLLISIONS

In this experiment only the lines at 8921 Å and 8933 Å were investigated. Intensity of the lines was graphed along the Y axis of the X-Y recorder. The X axis input was supplied by connecting its terminals in parallel with the Cambridge meter. This meant that the X axis was uncalibrated so, at short intervals, temperature as read on the meter was written in on the graph.

At the commencement of the experiment the low temperature oven which had not been switched on, was at the temperature of its surroundings. The monochromator was set at 8921 Å. The phase-sensitive detector time constant switch was set at "external" and two 45 mF capacitors were plugged into

the external time constant sockets. This gives a time constant of 45 s and a bandwidth of 0.074 Hz. The long time constant made adjustment of the wavelength drum a slow process. The wavelength was set by turning the drum to the approximate correct position and then rotating slowly back and forth to find the maximum intensity as indicated by the output meter of the phase sensitive detector. A small amount of backlash in the wavelength drum also contributed to the difficulty of setting wavelength.

The zero was set by cutting off radiation into the entrance slit by a piece of black paper. After this had been in position several minutes, the zero adjustment on the phase-sensitive detector was set so that the output meter showed zero. The black paper was then removed.

The experiment was begun by turning on the low-temperature oven and gradually increasing the temperature (by turning up the Variac in small steps at intervals). This process continued for 2¾ hours during which time the temperature increased from 41°C to 113°C. At this stage the monochromator was set on 8933 Å and the low temperature oven allowed

to cool slowly for 2¼ hours to 47°C.

The caesium vapour pressure was calculated as described in section 3.18 and the ratio of the intensities of the two lines was calculated from the Y-values on the graph.

4.9 CAESIUM-INERT GAS COLLISIONS

In this experiment the temperature of the low-temperature oven was set at a fixed temperature of about 90°C so that sufficient caesium atoms were present to give relatively intense fluorescence.

The fluorescent light was monitored as described in section 4.7 on the X-Y recorder. In this case the X-axis was connected to the output terminals of the capacitance manometer control unit so that intensity was recorded as a function of inert gas pressure.

At the start of the experiment the zero of intensity was adjusted as above and the monochromator was set at 8921 Å (this line being at its most intense at zero pressure of inert gas). The ion pump was switched off. The Granville-Phillips valve connecting the resonance cell to the ultra-high vacuum manifold was fully opened. The Granville-

Phillips valve connecting the relevant gas flask to the manifold was then opened slightly to allow inert gas to leak slowly into the manifold and thence into the resonance cell. A typical rate of flow was such that the rate of increase of pressure was about 0.2 torr min^{-1} in the case where pressure was allowed to vary from 0-20 torr; 1 torr. min^{-1} in the case where higher pressures were examined. When the pressure reached the highest value for the particular experiment, the two valves were closed, the diffusion pump switched on, and the isolation valve between the manifold and diffusion pump opened. As on every occasion on which the isolation valve was opened, the cold trap was immersed in liquid nitrogen.

At this stage the monochromator setting was changed to 8933 Å and the zero of intensity checked. The resonance cell was then opened to the diffusion pump and the inert gas pumped out (together with some of the caesium) to a pressure of less than 10^{-3} torr. (That sufficient caesium was left in the resonance cell was checked later by noting that condensed caesium still remained in the bottom of the cell at the temperature of the experiment.) The resonance cell valve was then closed and the isola-

tion valve immediately afterwards. After a short period to allow the system to stabilize, the inert gas was admitted as before.

When the maximum pressure for the particular experiment was again reached, the monochromator was set at 6985 Å and the procedure of the preceding paragraph repeated. At the end of the experiment the gas was removed as described in section 4.5.

The capacitance manometer was operated on its most sensitive range (nominal 10 torr f.s.d.) with the oil manometer set at 10 torr. This enabled a range of 0-20 torr to be measured. For higher pressure the manometer was operated on the next most sensitive range (100 torr f.s.d.) with 10 torr at the oil manometer as a reference pressure.

5. RESULTS AND DISCUSSION

5.1 FLUORESCENT SPECTRUM

Four scans of the fluorescent spectrum were made using the procedure described in section 4.7. The conditions inside the resonance cell during each of the scans were (a) no foreign gas, 3.6×10^{-5} torr caesium vapour, resonance cell temperature 214°C; (b) no foreign gas, 5.7×10^{-4} torr caesium vapour, temperature 219°C; (c) 0.7 torr argon, 2.4×10^{-4} torr caesium vapour, temperature 234°C; and (d) 20 torr argon, 2.3×10^{-4} torr caesium vapour, temperature 230°C. The spectra obtained are shown in figures 5.1(a), 5.1(b), 5.1(c), and 5.1(d) respectively. (The term "no foreign gas" means less than 10^{-8} torr of foreign gas present.)

The time constant used on the phase-sensitive detector was 3 sec so that the detector system could keep up with the scanning motor on the monochromator. This was still too slow a time constant to enable certain spectral lines to be resolved as explained earlier. With this time constant, the noise bandwidth of the system was 0.11 Hz.

In order to observe the caesium spectrum it was

Figs. 5.1 - Caesium Fluorescent Spectra.
(Wavelengths are in Å and refer to
caesium lines unless otherwise indicated.)

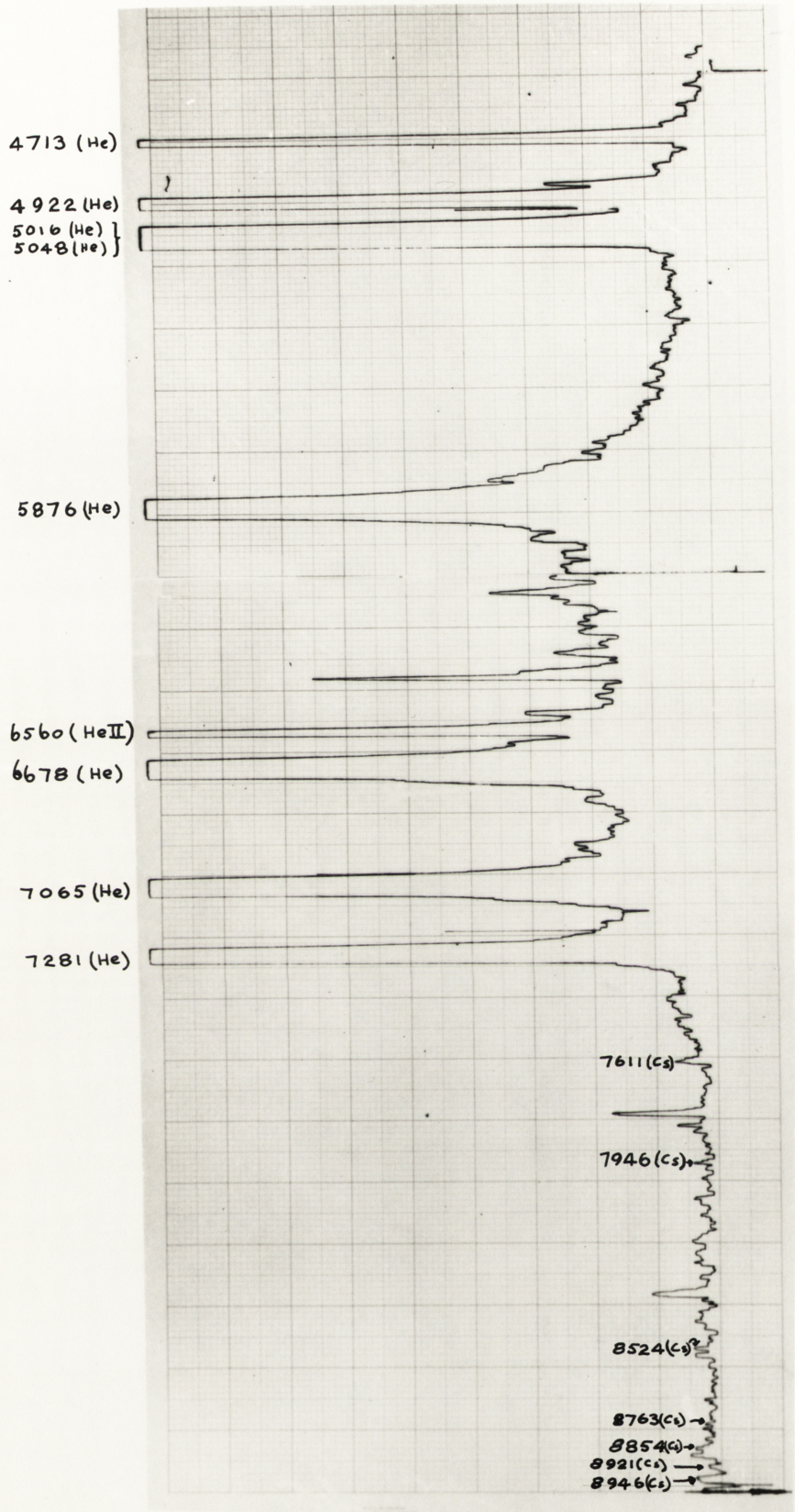

Fig. 5.1(a) - Caesium Fluorescent Spectrum (59°C)

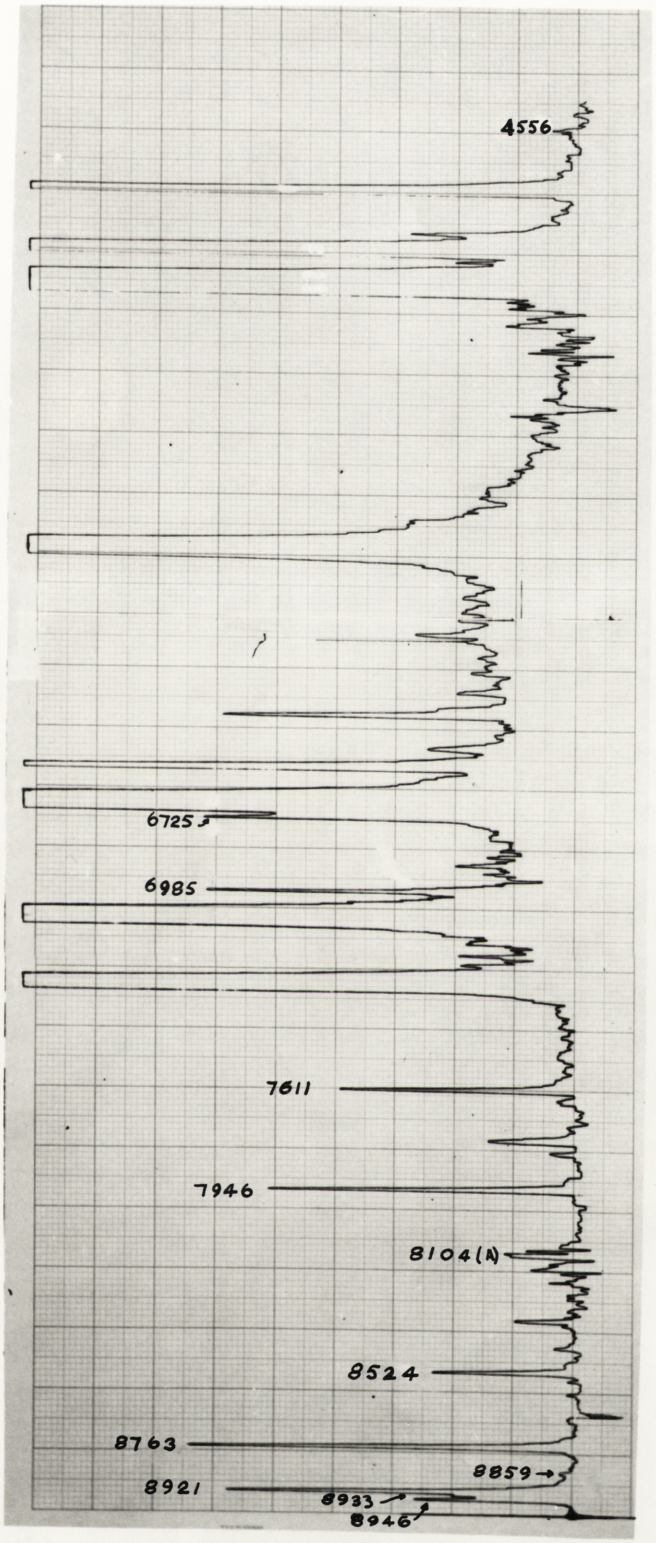

Fig. 5.1(b) - Caesium Fluorescent Spectrum ($100^{o}C$)

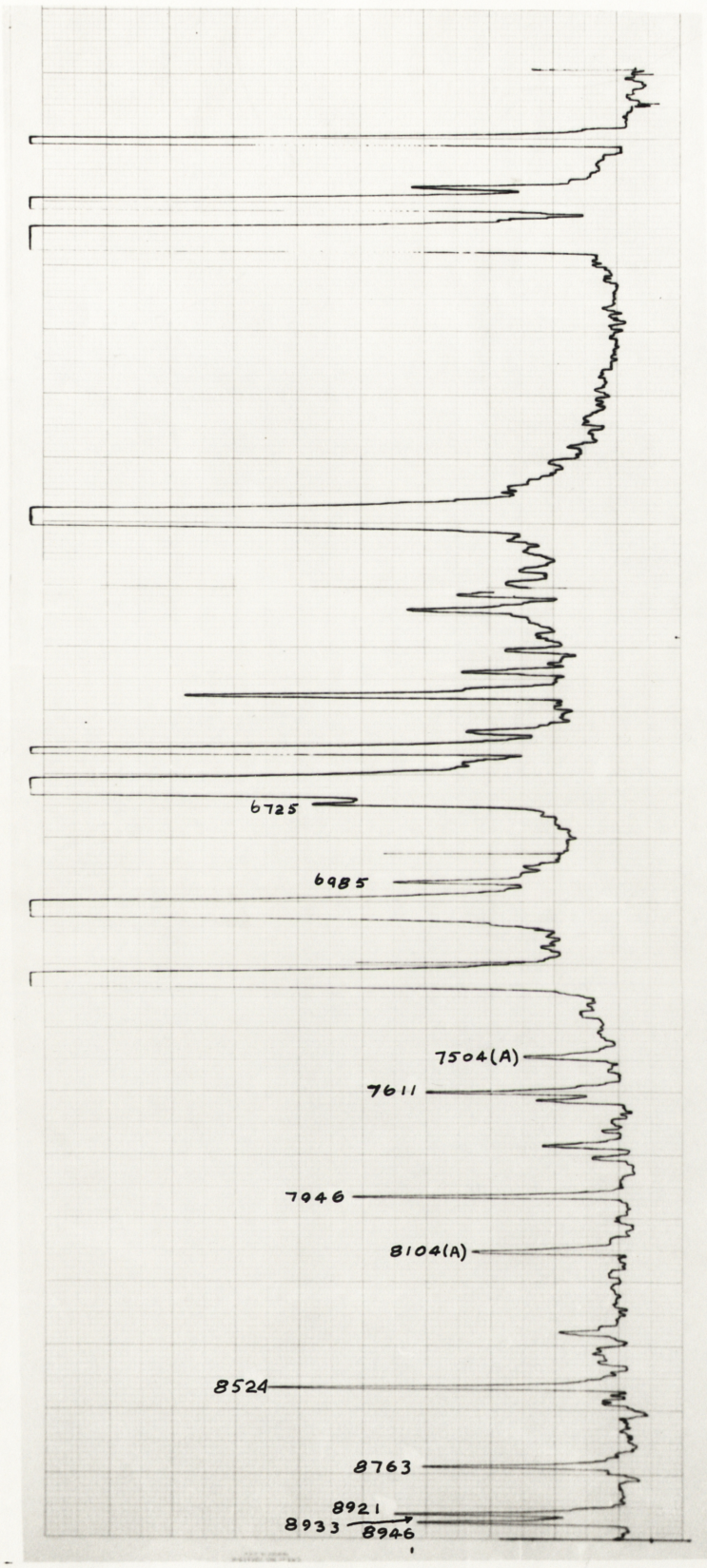

Fig. 5.1(c) - Caesium Fluorescent Spectrum (0.7 torr Argon)

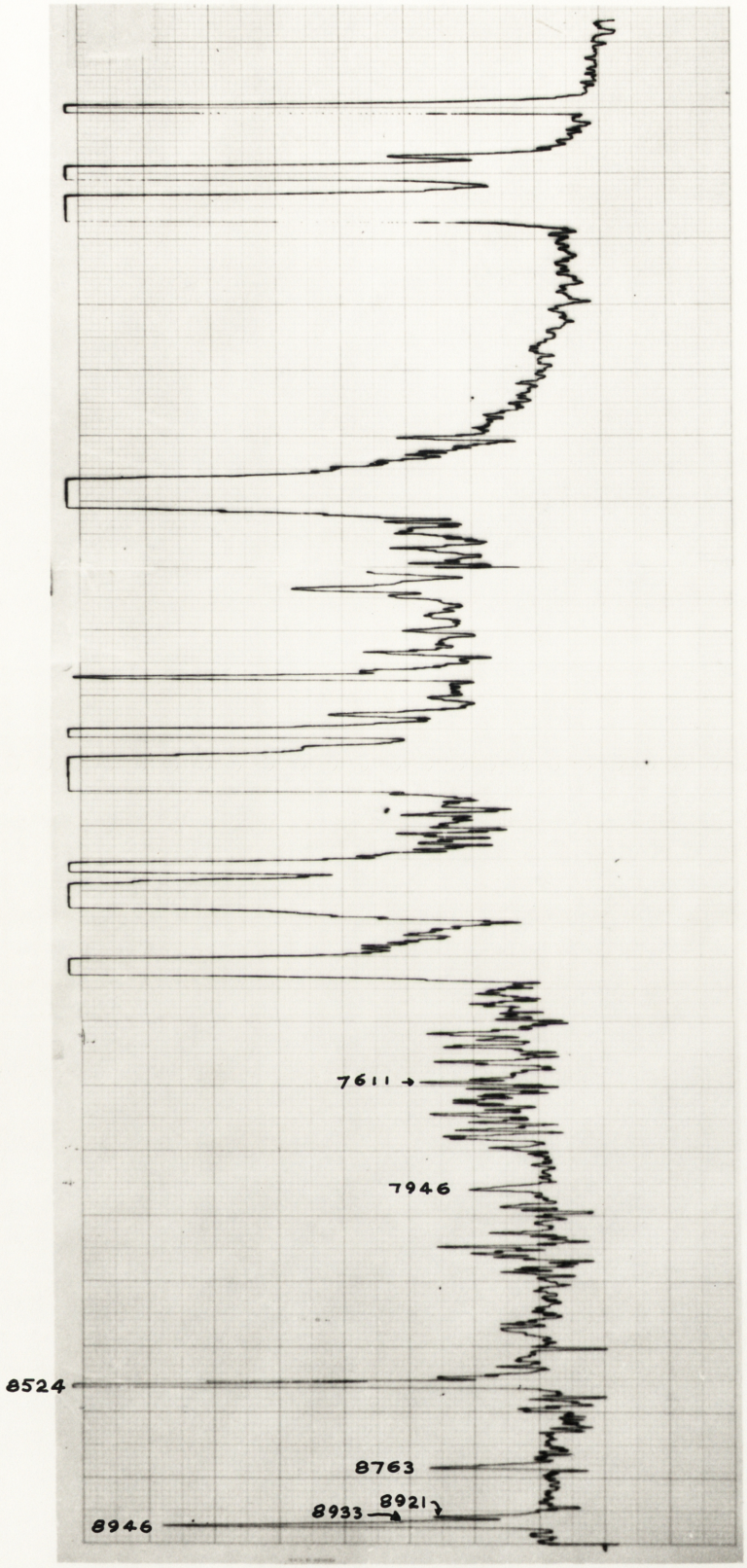

Fig. 5.1(d) - Caesium Fluorescent Spectrum (20 torr Argon)

necessary to use the low-noise amplifier at full amplification. This resulted in some of the helium lines being too strong to fit onto the graph paper of the recorder. The helium light was much more intense than the caesium light although in a few instances caesium lines were also too intense to fit on the graph paper.

There exists in this series of experiments a difficulty in obtaining any quantitative results. Owing to the speed of scanning, in relation to the time constant of the detector, a number of lines lie on the wings of more intense helium lines. A number of other lines are so weak as to be almost buried in noise.

In Figure 5.1(a) all of the prominent spectral lines belong to the helium spectrum with a couple of exceptions which could not be identified due to the difficulty of reading wavelength exactly which was noted in section 3.17. These few lines were assumed to belong to the helium lamp because they remained relatively constant for different conditions in the resonance cell. The only caesium lines that can be detected with any degree of cer-

tainty are 8946 Å ($6P_{1/2} \rightarrow 6S$), 8921 Å ($8P_{1/2} \rightarrow 5D_{3/2}$), 8763 Å ($6D_{3/2} \rightarrow 6P_{1/2}$), 8524 Å ($6P_{3/2} \rightarrow 6S$), 7946 Å ($8S \rightarrow 6P_{3/2}$), and 7611 Å ($8S \rightarrow 6P_{1/2}$). The line at 6985 Å ($7D_{3/2} \rightarrow 6P_{3/2}$) is possibly also there but it is difficult to be positive about this. This is basically in agreement with Boeckner's[1] observations. The transitions $7P_{3/2} \rightarrow 6S$ and $7P_{1/2} \rightarrow 6S$ (4556 Å and 4594 Å respectively) were not able to be identified with any certainty although these lines are prominent in the caesium arc spectrum. This may be explained by the lines being just below the low wavelength cut-off of the Wratten filter which is very sharp according to the manufacturer. There is no real reason to suppose that radiative transitions from the 7P states do not occur if one considers the cascade process $8P_{1/2} \rightarrow 8S_{1/2} \rightarrow 7P$. This process is reasonably probable according to the relevant branching ratios (see Appendix I). The fact that these lines did not become noticeable in any of the scans probably indicates that the filter cut-off is as good as the manufacturer states.

When the caesium vapour pressure was increased by a factor of about ten (Figure 5.1(b)), all of

the lines seen earlier appear but much more strongly. At this pressure, however, the lines 8933 Å ($8P_{3/2} \rightarrow 5D_{5/2}$), 6985 Å ($7D_{3/2} \rightarrow 6P_{3/2}$), and 6725 Å ($7D_{3/2} \rightarrow 6P_{1/2}$) are quite definitely present. The line 6975 Å ($7D_{5/2} \rightarrow 6P_{3/2}$) may also be present though overshadowed by its neighbour 6985 Å. Its presence is therefore not definite. The appearance of these three lines indicate that the levels $8P_{3/2}$ and $7D_{3/2}$ are being populated through collisions of the second kind between excited caesium atoms in the $8P_{1/2}$ state and ground state caesium atoms, the extra energy needed for excitation coming from the kinetic energy of the atoms. It also appears that the $7D_{5/2}$ level is not being very much excited if at all.

The increase in intensity of the caesium lines is very much in keeping with the interpretation that the increase is due simply to the increased density of caesium atoms. This being the case it is reasonable to assume that the lines originating from the $7D_{3/2}$ level were present in Figure 5.1(a) but simply obscured. Boeckner was unable to detect any signs of emission from the 7D levels even though he had a caesium vapour pressure of $\sim 10^{-3}$ torr. If it is

assumed that all allowed radiative transitions occur in the cascades from the excited states to the ground state, then the situation must be as shown in Figure 5.2.

The occurrence of excitation of 7D levels meant that the original aim of the experiment had to be modified (see section 1.5). The simple process originally expected whereby only the $8P_{3/2}$ level was excited collisionally was now known to be complicated by the occurrence of extra processes. Due to the sequence in which experiments were performed and to the time limit on the experiments, insufficient data was collected in the case of caesium-caesium collisions to be of much value.

The scans of the fluorescent spectrum with argon present in the resonance cell were done at different times from those where only caesium was present. These two scans were performed with different conditions prevailing (caesium vapour pressure, temperature of resonance cell, etc.) since the apparatus was such that exact reproduction of conditions was not possible. Hence each of the fluorescent spectra shown in Figures5.1 was recorded with slightly different conditions of temperature

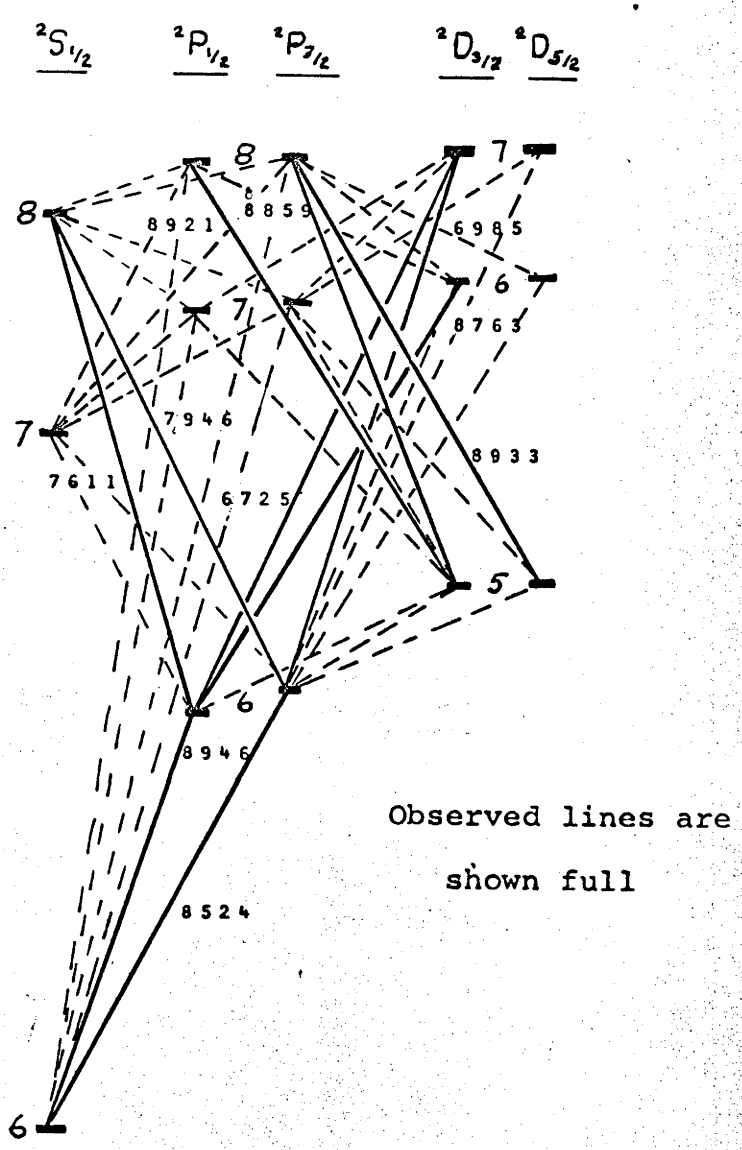

Fig. 5.2 - Caesium Transitions Occurring

prevailing in the resonance cell. For this reason exact comparisons between the spectra are not possible but some broad observations can be made.

With 0.7 torr of argon and 2.4×10^{-4} torr of caesium present in the resonance cell, the spectrum is as shown in Figure 5.1(c). The appearance of two distinct lines identified as belonging to the neutral argon spectrum (8104 Å and 7504 Å) is attributed to impurities present in the helium lamp. This is assumed because the 8104 Å line apparently exists in one of the caesium fluorescent spectra (Figure 5.1(b)). That the helium lamp was not properly constant was obvious since it had frequently to be refilled. The spectra in Figures 5.1(a), 5.1(b), and 5.1(c) were obtained with the same charge of helium in the lamp (a) being obtained soon after filling, (b) a couple of hours later, and (c) about one day later. The spectrum in Figure 5.1(d) was obtained after the helium lamp had been refilled. In this last case the change in background noise is probably due to the difference in the helium lamp.

The major changes in the spectrum are the relative increases in the intensities of the lines

8946 Å ($6P_{1/2} \rightarrow 6S_{1/2}$) and 8524 Å ($6P_{3/2} \rightarrow 6S_{1/2}$). The enhanced population of the 6P levels indicated that the $7D_{3/2}$ level is being populated to a greater extent since the chief modes of decay of this level are via the 6P levels (and also the 7P levels). A relative reduction in intensity of the line 8763 Å ($6D_{3/2} \rightarrow 6P_{1/2}$) implies that the enhanced population of the 6P levels is not via 6D levels which would be populated by radiation from 8P levels. Hence it is assumed that 8P populations have been reduced. The only other observable radiation populating the 6P levels is from the 8S level (7611 Å and 7946 Å). Since neither of these lines was intensified, it is assumed that the stepwise decay 8P→8S→6P was not responsible for enhancement of the 6P population.

This is not confirmed very well by the apparent intensity of the direct transitions from the $7D_{3/2}$ level (6985 Å and 6725 Å). The spectrum in Figure 5.1(d), however, does provide evidence that this is the trend. The addition of extra argon causes large relative increases in the intensities of the lines 8946 Å ($6P_{1/2} \rightarrow 6S_{1/2}$), 8524 Å ($6P_{3/2} \rightarrow 6S_{1/2}$), 6985 Å ($7D_{3/2} \rightarrow 6P_{3/2}$), and 6725 Å ($7D_{3/2} \rightarrow 6P_{1/2}$). (The

last named line overlaps the 6678 Å line of the helium spectrum.)

On the whole, then, these observations agree with those of Boeckner with the main difference being the observation of emission from the $7D_{3/2}$ level even when no inert gas is present. (It is worth noting that Boeckner used helium as the inert gas for his experiment.)

It is important to note here a detail which was not observed in any of the scans of fluorescent spectra. The reference is to the line at 6975 Å corresponding to the transition $7D_{5/2} \rightarrow 6P_{3/2}$. This transition has a transition probability slightly larger than that for the transition $7D_{3/2} \rightarrow 6P_{1/2}$ (6725Å) and if complete collisional mixing were the case the populations of the two 7D levels would be about the same order of magnitude so that the 6975Å line should appear with an intensity about the same as the 6725 Å line. It is assumed therefore that, under the conditions for which the fluorescent spectra were scanned, collisional mixing of the two 7D levels is at least not significant. This point will be further discussed in section 5.3.

5.2 CAESIUM-CAESIUM COLLISIONS

As mentioned in sections 4.8 and 5.1, only the lines 8921 Å and 8933 Å were observed in this experiment. It is not possible to draw many conclusions from the results obtained since at low caesium vapour pressures, where it is expected that collisional transfer of excitation between the two 8P levels is the dominant process, the intensity of the 8933 Å line was very low and noise effectively obscured much of the signal. It appears that the 8921 Å line increases continuously with caesium pressure. This indicates that excitation transfer away from the $8P_{1/2}$ level is not as probable as radiative decay in the pressure range observed. On the other hand, the intensity of the 8921 Å line increases at first with caesium density as excitation is transferred to the $8P_{3/2}$ level and then levels off somewhat, presumably as the transfer of excitation to 7D levels becomes important. It then proceeds to increase further as caesium density increases, probably due to increased transfer of excitation from a greater number of radiatively excited ($8P_{1/2}$) caesium atoms.

5.3 CAESIUM-INERT GAS COLLISIONS

In these experiments three lines were observed separately as described in section 4.9. These were 8921 Å ($8P_{1/2} \rightarrow 5D_{3/2}$), 8933 Å ($8P_{3/2} \rightarrow 5D_{5/2}$), and 6985 Å ($7D_{3/2} \rightarrow 6P_{3/2}$). Since the energy gap between the two 7D levels is 21 cm^{-1} compared with 83 cm^{-1} for the gap between the two 8P levels it was assumed for ease of calculation that the two 7D levels could be treated as one 7D level.

The process to be treated then is one in which caesium atoms in the ground ($6S_{1/2}$) state are excited to the $8P_{1/2}$ level by irradiation with 3889 Å light from a helium lamp. Collisions may cause some of the excited atoms to be further excited to the $8P_{3/2}$ level or the 7D level. Collisions may be with unexcited caesium atoms in which case the excitation may be transferred or with atoms of an inert buffer gas which remain unexcited. The former collisions are comparatively rare and may be ignored when more than about one torr of buffer gas is present. Collisions between two excited caesium atoms are even rarer and may be ignored at all times.

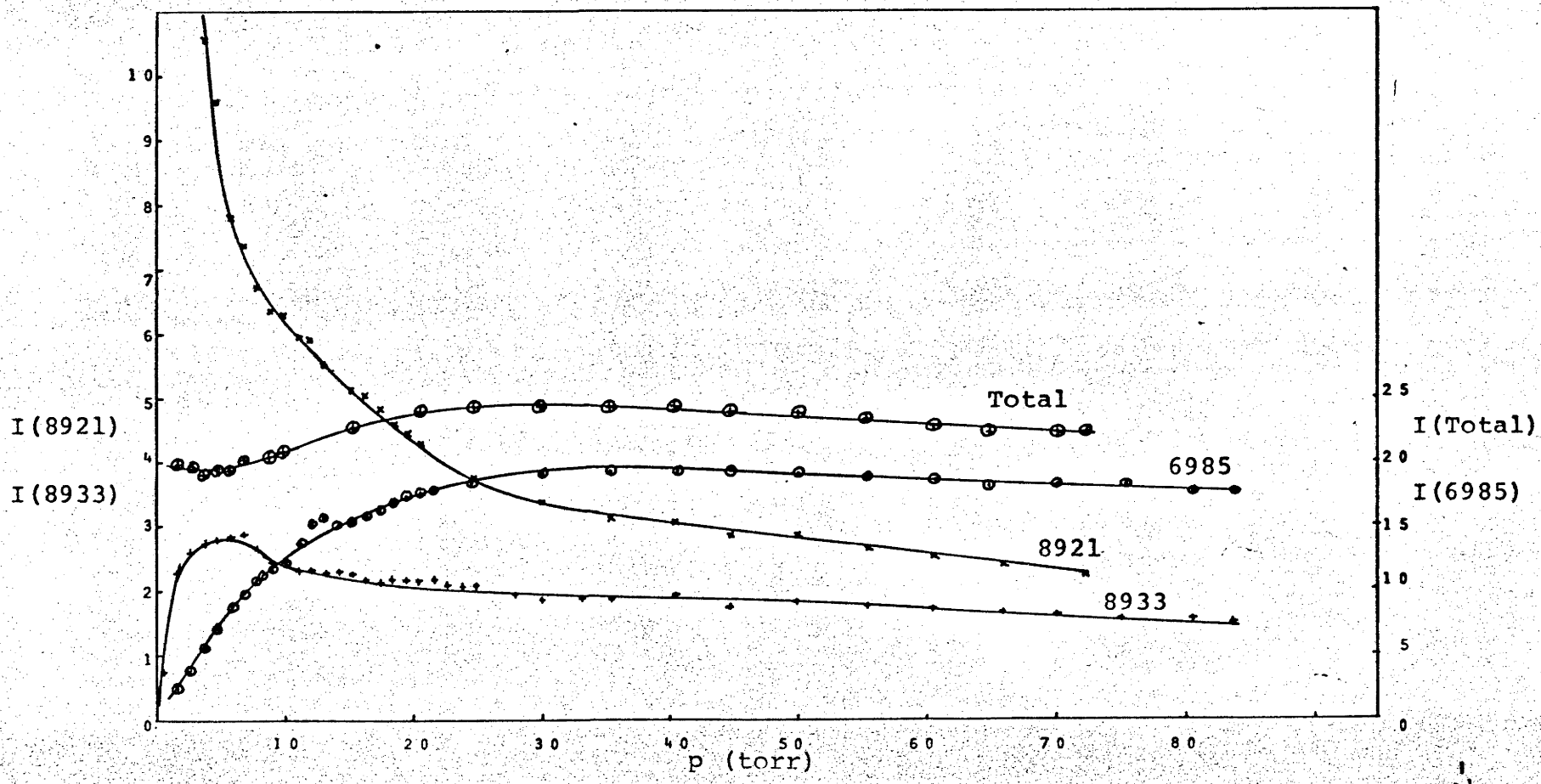

Fig. 5.3(a) - Caesium-Argon

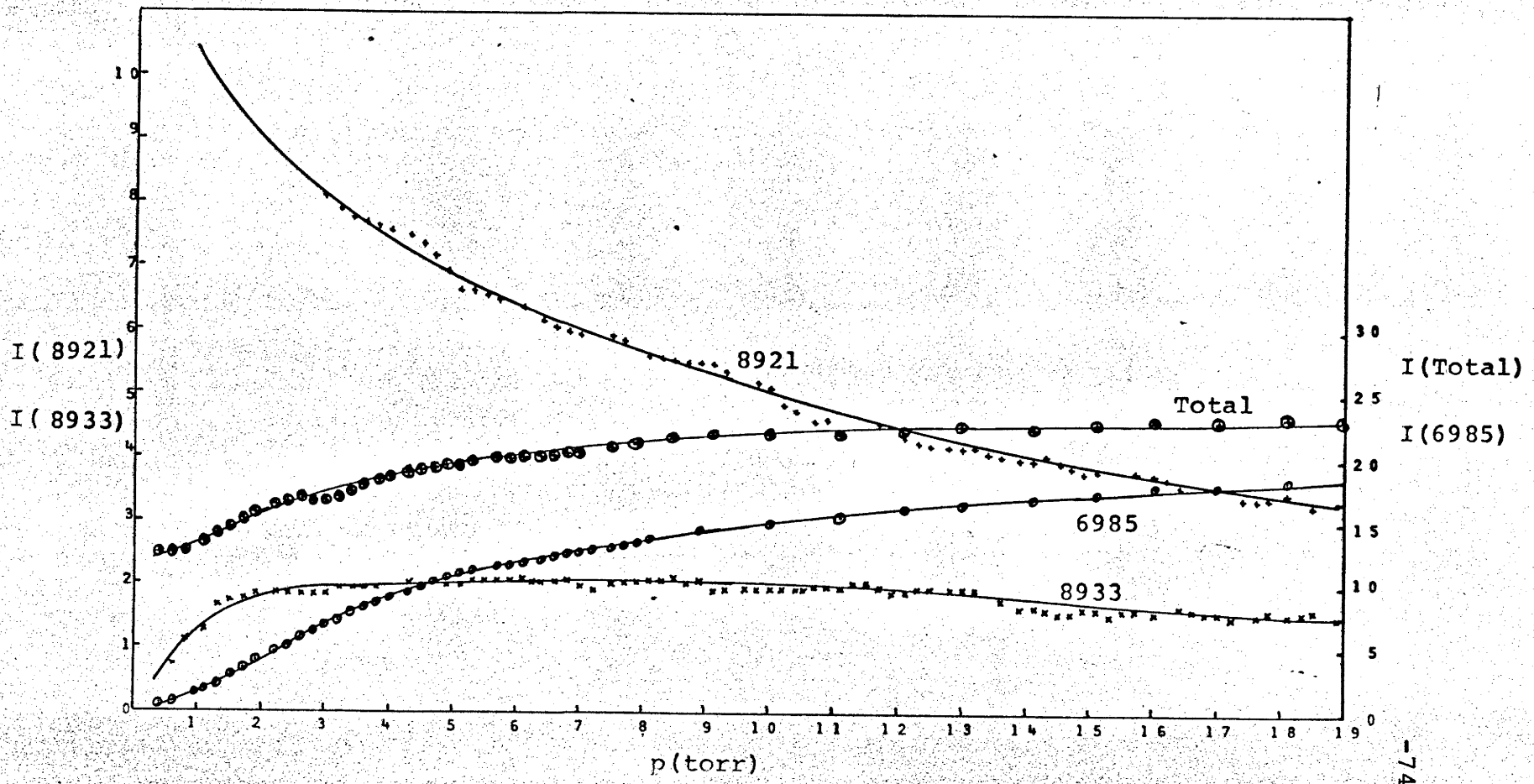

Fig. 5.3(b) - Caesium-Argon

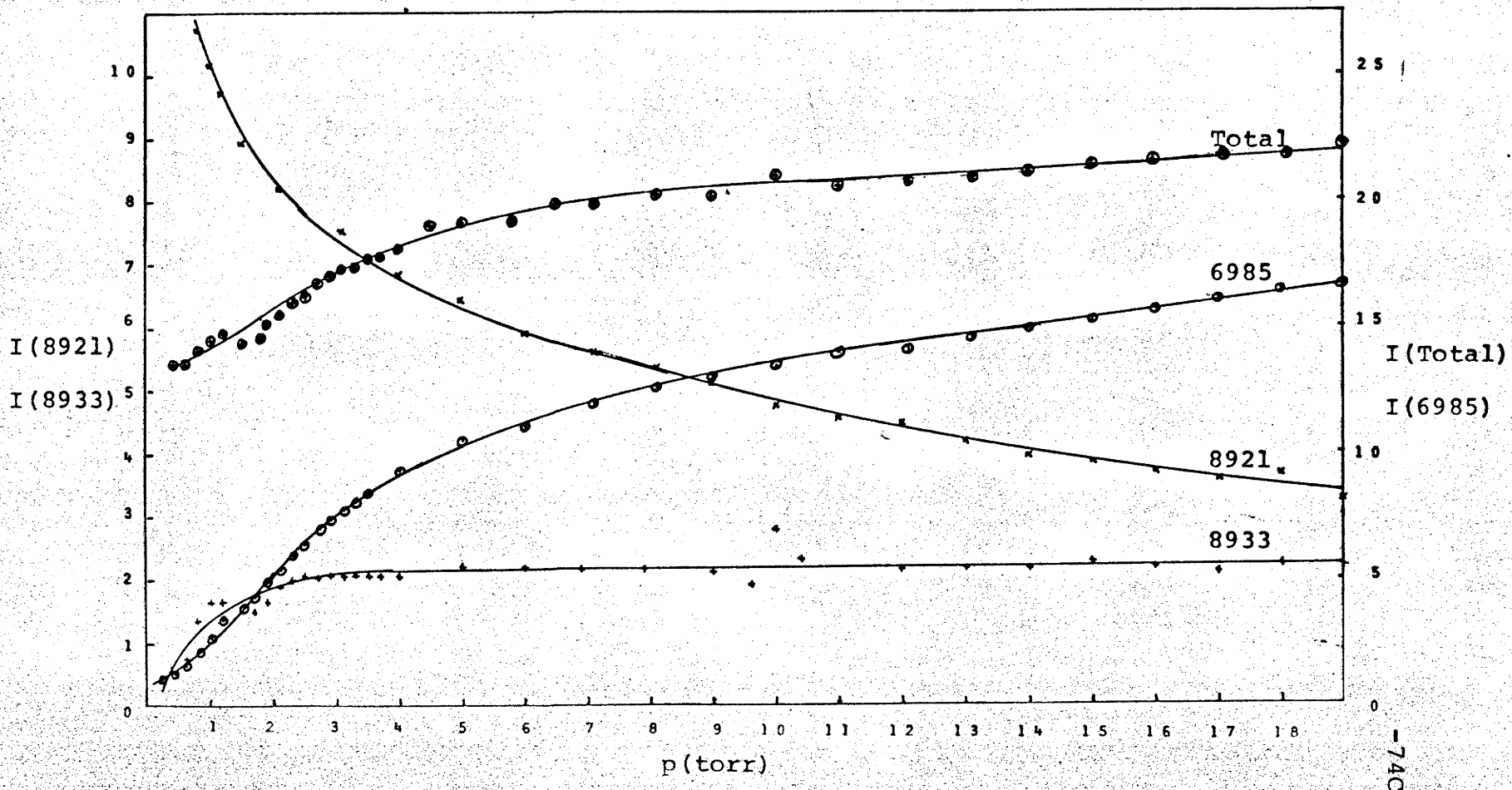

Fig. 5.3(c) - Caesium-Krypton

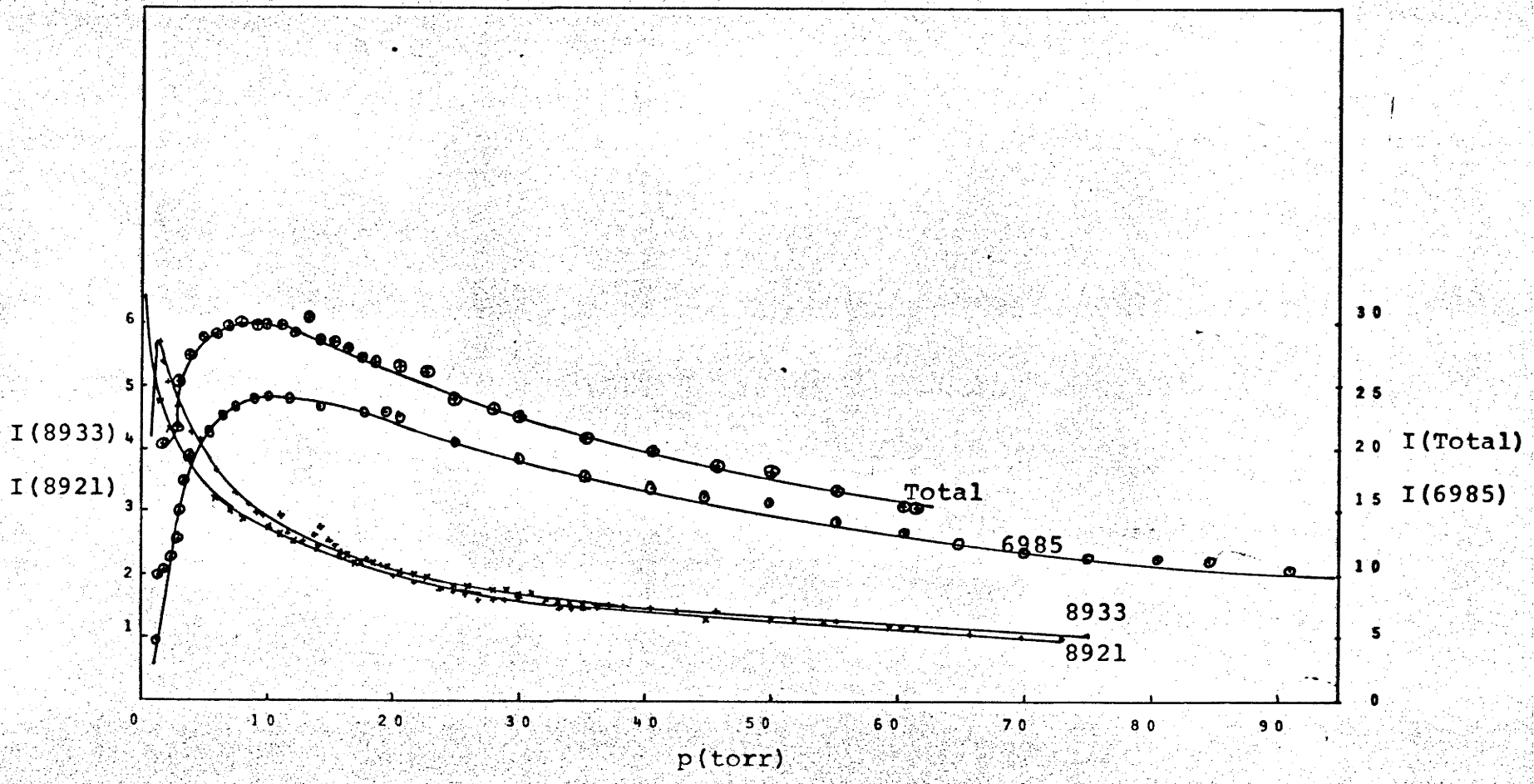

Fig. 5.3(d) - Caesium-Helium

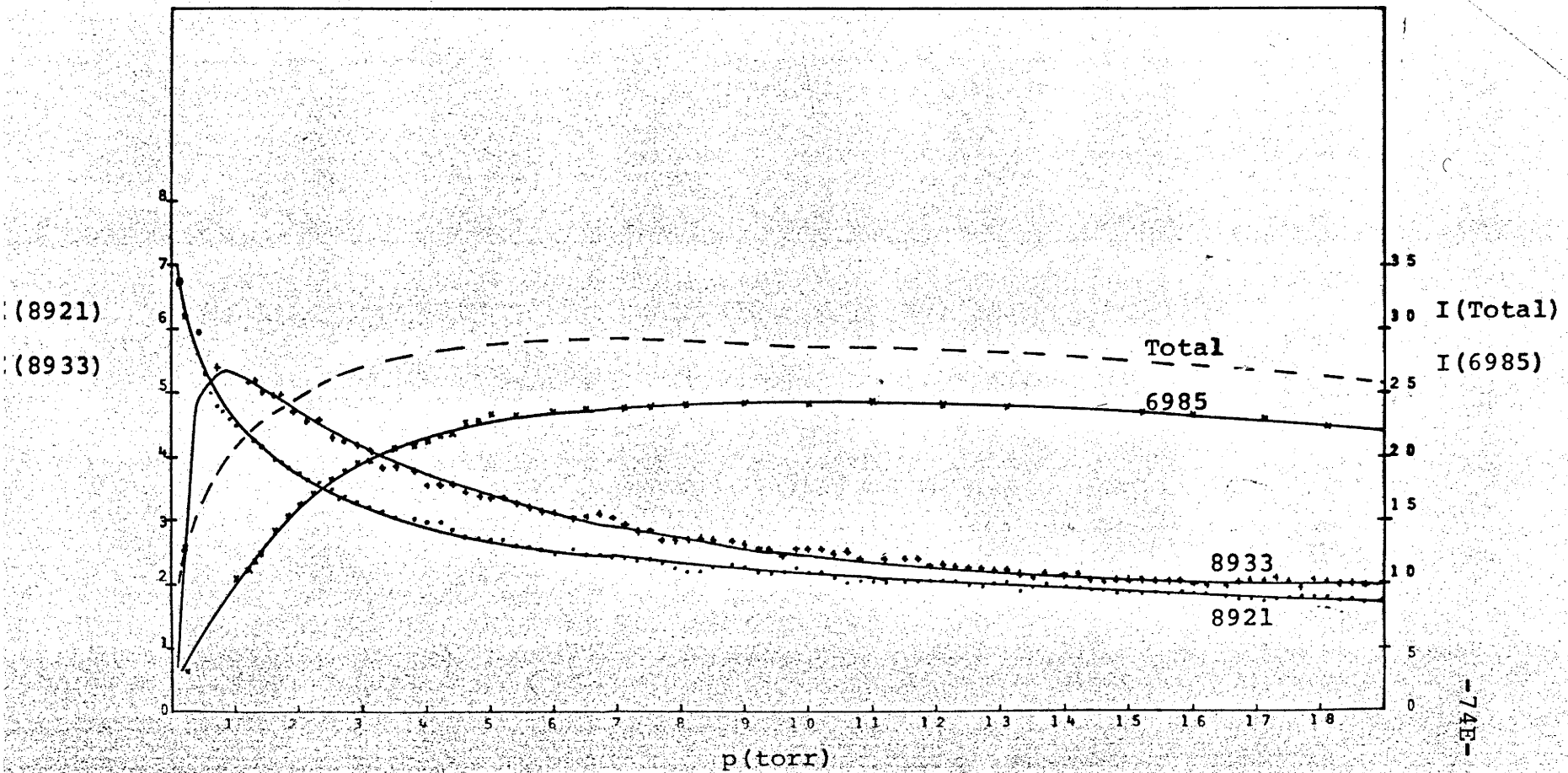

Fig. 5.3(e) - Caesium-Helium

The results reproduced in Figures 5.3(a), (b), (c), (d), and (e) are not direct copies of the output of the X-Y recorder. The graphs obtained from the X-Y recorder are not in a form suitable to be copied as the curves are in segments due to switching between different amplification levels of the detection system so that as much detail as possible could be collected. The graphs shown in the various Figures 5.3 are plotted from the results taken from the X-Y recorder output corrected for spectrophotometer sensitivity. An extra curve has been added to these figures, that showing total fluorescence observed. This is simply the sum of the other three curves. (It should be noted that two scales are used for intensity.)

Looking first then at the curves for total intensity it was observed that at low pressures of inert gas the curves show an increase of total intensity with pressure. This is interpreted as being due to an increase of the width of the caesium absorption line as a result of Lorentz Broadening. The effects of such broadening have been remarked upon by Gould[7]. A comparison of Figure 1.2 with

the hypothetical case (1) given on page 194 of Mitchell and Zemansky[3] indicates how such broadening could be effective.

In those cases where the inert gas pressure becomes high enough, the total fluorescent intensity is seen to reach a maximum as pressure is further increased and then to begin decreasing. It is assumed that this is due to further sensitized fluorescence which was not observed in any part of the experiment i.e. the curve representing total fluorescence is lacking in one component. This point will be discussed later in this section.

The terms "low pressure" and "high pressure" have been used in this discussion with no indication as to their definitions. It should be noted that the terms have different meanings in connection with different buffer gases. For example, "high pressure"in the case of helium may still be "low pressure" for the same pressure of argon. The terms are defined solely in relation to the effects observed.

The general shapes of the curves for the variation of intensity with pressure of the three lines

8921 Å, 8933 Å, and 6985 Å are the same for each of the experimental runs. The 8921 Å curve decreases from some high value at low pressure as pressure of inert gas increases. The intensity at zero pressure would depend on the caesium vapour pressure but not in a simple way. In general the higher the vapour pressure, the greater the absorption of helium light and the stronger the emission of fluorescent light. However, higher vapour pressure of caesium also means greater transfer of excitation through collisions of the second kind with other caesium atoms which thus reduces the fluorescent light at this wavelength.

The 8933 Å line starts at low pressure from a low level which would be zero but for the fact that some population of the $8P_{3/2}$ level occurs through caesium-caesium collisions. As pressure of inert gas increases so does the intensity of the 8933 Å line until at some pressure a maximum is reached. Thereafter the intensity decreases as pressure increases rather as the 8921 Å line did. In some of the experimental runs the pressure of inert gas never became high enough for the decrease or even

the maximum to be clearly evident.

The shape of the intensity vs. pressure curve for the 6985 Å line is best described as increasing with an S-shape from a low level which would be zero but for caesium-caesium collisions. The S-shape of the curve at low pressure is really only evident in those experimental runs where the low pressure region of inert gas extends to higher actual pressures. In these cases, however, the high pressure behaviour of this curve is not seen. At high pressures this curve reaches a maximum and then decreases as pressure increases in much the same way as did the 8933 Å line. The maximum for the 6985 Å line was always at a higher pressure than that for the 8933 Å line in the same experimental run.

To explain the behaviour of these curves, it is useful to turn to the theory of chemical kinetics. In particular one considers the simple reaction $A \rightarrow B \rightarrow C$ as is discussed in the books by Laidler[18] (p.22) and Kondrat'ev[19] (p.20). Both of these texts derive the rate equations for these reactions

and solve them exactly. The resultant curves depicting the concentrations of A, B, and C as functions of time have similar shapes to those described above, obtained when the intensities of the lines 8921 Å, 8933 Å, and 6985 Å respectively are plotted against pressure. An obvious difference between the two situations is that whereas the concentrations of A and B approach zero, the intensities of the lines 8921 Å and 8933 Å do not. This is clearly due to the reversibility of the reactions in this experiment.

The S-shape of the curve representing the concentration of C is explained as being due to there being an intermediate substance (in this case B) formed from which C is in turn formed. This is because the rate of formation of C is proportional to the concentration of B. Hence at zero time the rate of formation of C is zero since concentration of B is then zero. The rate of formation of C increases with concentration of B and hence the S-shaped curve for C. The existance of a so-called induction period is stated to be an indication that

C is formed from A via some intermediate substance. This gives a clue to the course of the reactions being observed in this experiment.

If a similar argument is now applied to the experiment reported here it is clear that the reaction being observed is $6S_{1/2} \rightarrow 8P_{1/2} \overleftrightarrow{} 8P_{3/2} \overleftrightarrow{} 7D_{3/2}$. (The reason for the choice of subscript for the 7D level will be discussed later.) The process described earlier in this section is incorrect then to the extent that the excitation transfers $8P_{1/2} \overleftrightarrow{} 7D_{3/2}$ cannot occur (or can hardly occur.) The $8P_{3/2}$ level is an intermediate state in the reaction similar to B in the above discussion.

Consideration of the theory developed in Chapter 2 becomes very difficult quite quickly. For example, differentiation of the equation (2.18) to determine if the curve for n_2 should have a peak leads to an equation with a number of unknown constants which is difficult to interpret. The following simple argument should show, to a first approximation, at least, that the process assumed is correct.

It is assumed that only collisions with inert gas atoms cause excitation transfer and that a region of pressure near to zero is considered so that, to a first approximation, the concentration of n_1 may be assumed constant. As pressure increases from zero, the concentration of n_2 is given by $k_{12}a\ n_1$ which is proportional to pressure (or concentration) of inert gas. If n_2 is plotted against pressure, a straight line through the origin results. Similarly, for the assumed process,

$$n_3 = k_{23}n_2a$$
$$= k_{23}k_{12}n_1a^2$$

so that a graph of n_3 plotted against pressure would look like a parabola near the origin and have zero slope there. This fits the observed shape of the graph. If n_3 were formed directly from n_1 then it would also have a linear graph near the origin which would be expected to be noticeable, other effects being equal, because at low values of a, a value of n_3 proportional to a would be larger than one proportional to a^2. So if the process $n_1 \rightarrow n_3$ occurred at all it was assumed negligible in

the theory developed in Chapter 2.

There is a further complication that was hinted at in the last paragraph of section 5.1 and mentioned explicitly earlier in this section. This is the behaviour of the 6985 Å curve at high pressure. It was pointed out earlier in this section that the curve decreases at high pressure rather like the 8933 Å curve. From the previous discussion it seems quite obvious that the $7D_{3/2}$ level is also an intermediate level in the population of some other level just as the $8P_{3/2}$ level is in the formation of the $7D_{3/2}$ level.

If the zero of energy is set at the $8P_{1/2}$ level, then the energy values of the various relevant energy levels are[8]:

$8P_{3/2}$	-	82 cm^{-1}
$7D_{3/2}$	-	339 cm^{-1}
$7D_{5/2}$	-	360 cm^{-1}

The next highest energy level is $9S_{1/2}$ at 1202 cm^{-1}. So if the energy differences alone are considered it seems strange that the $7D_{5/2}$ level is not populated as was pointed out in section 5.1.

It appears, therefore, that the decrease in intensity of the 6985 Å line is due to the $7D_{5/2}$ level's being populated via the $7D_{3/2}$ level and not directly (or at least only slightly) from the 8P levels. This is the reason for the choice of subscript made earlier. This being the case, the dominant process occurring must be:

$$6S_{1/2} \rightarrow 8P_{1/2} \rightleftarrows 8P_{3/2} \rightleftarrows 7D_{3/2} \rightleftarrows 7D_{5/2}$$

where each of the excited levels can also decay radiatively and other processes occurring are considered as being negligible. The behaviour of the $7D_{5/2}$ level was not observed (e.g. by monitoring the behaviour of the 6975 Å line ($7D_{5/2} \rightarrow 6P_{3/2}$)) because this type of behaviour was not suspected until it was too late. However, it seems reasonable to discount any further collisional transfer of excitation to the next energy level ($9S_{1/2}$) because of the large energy defect (~3.5 kT at 500°K). An explanation of the non-appearance of the 6975 Å line in any of the scans of the fluorescent spectra described in section 5.1 is that the inert gas pressure was not high enough to bring about significant population of the $7D_{5/2}$ level. The higher rate of radiative decay of the $7D_{3/2}$ level com-

pared with the rates of the 8P levels (~three times faster) means that the rate constant k_{34} would need to have three times the value of k_{12} for transfer between the 7D levels to be as evident as that between the 8P levels; alternatively, the effects of 7D mixing would become evident at pressures about three times that at which the effects of 8P mixing are noticed if k_{34} is about equal in value to k_{12}.

In the notation of Chapter 2, $k_3 < k_{34}a$ for significant population of the $7D_{5/2}$ level. This explains the reason for the particular process which was considered in Chapter 2 and also the approximation made in disregarding excitation transfer to the $7D_{5/2}$ level to obtain equations (2.30) and (2.31). The decrease in "total" fluorescent intensity noted towards the beginning of this section is also explained by this hypothesis.

Some calculations of the simple system involving only three excited states were performed to check on some of the properties expected of the rate constants involved. It was assumed that the lifetimes of the states 1 and 2 were equal to each other and about one-third that of state 3 which corresponds approximately to the $8P_{1/2}$, $8P_{3/2}$, and $7D_{3/2}$ states of caesium.

Various values of rate constants were tried in the equations for this system and it was found that the population of state 2 had a maximum value if the ratio k_{23}/k_{12} was less than 3. As the ratio approached 3 (the ratio of the lifetimes) the maximum moved to higher pressure. (The rate constants were chosen $k_{12} = k_{21}$ and $k_{23} = k_{32}$ for this calculation.) Further calculations in which all the rate constants were different showed that the maximum tended to be sharper if $k_{23}>k_{32}$ and had a greater value if $k_{12}>k_{21}$. The rate constants determined from the results fitted roughly this description. The values of k_{12} and k_{21} for caesium-helium collisons were roughly an order of magnitude greater than those for argon and krypton whereas the values of k_{23} and k_{32} were all about the same order of magnitude. This indicates that the prominent maxima in the case of collisions with helium are due to the higher relative velocity in these cases.

To calculate the cross-sections, the ratios R and R' defined in equations (2.47) and (2.51) were calculated and plotted as a function of the inverse of the inert gas pressure. Some of these graphs are shown in Figures 5.4(a), (b), (c), (d), and (e)

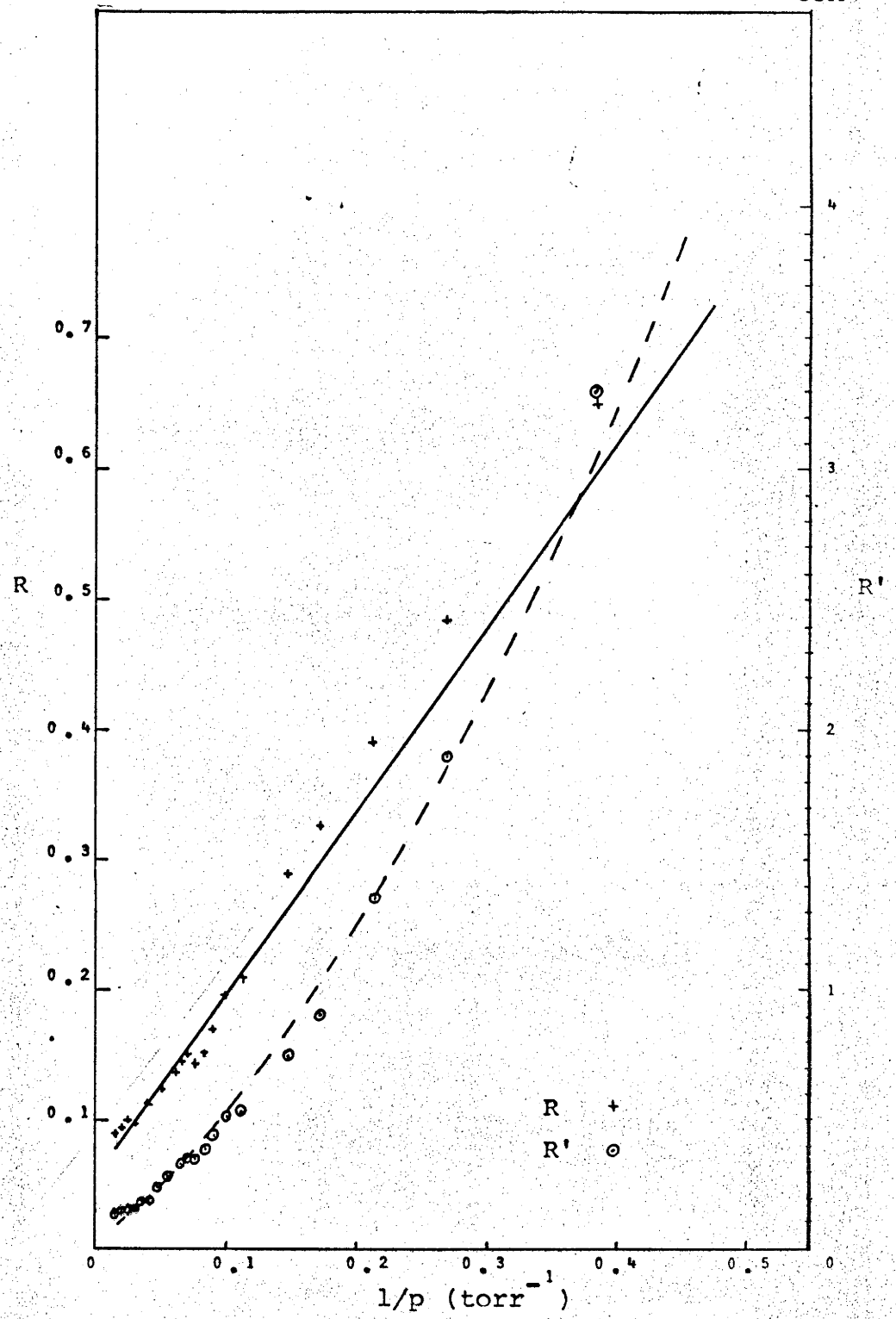

Fig. 5.4(a) - Caesium-Argon

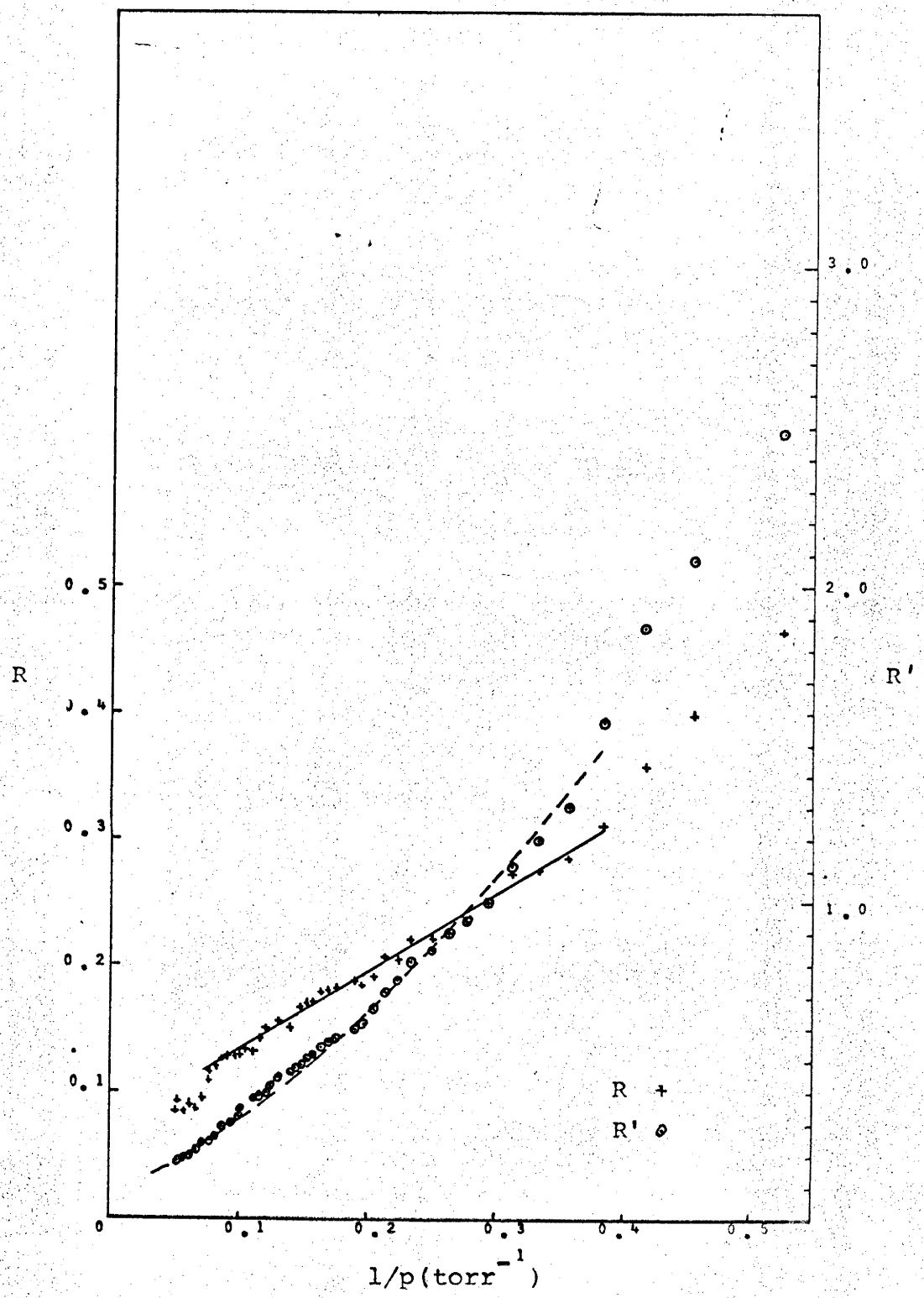

Fig. 5.4(b) - Caesium-Argon

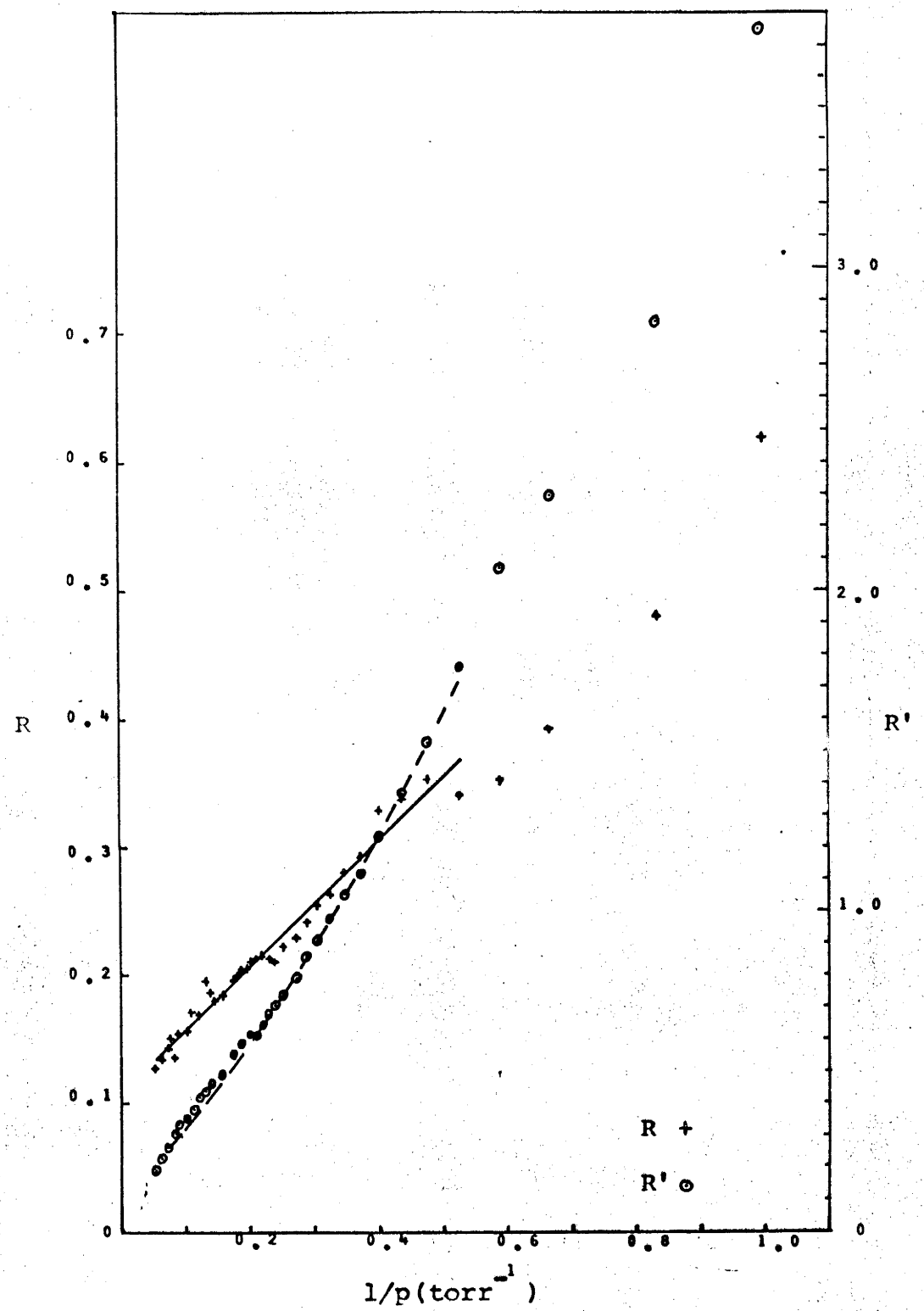

Fig. 5.4(c) - Caesium-Krypton

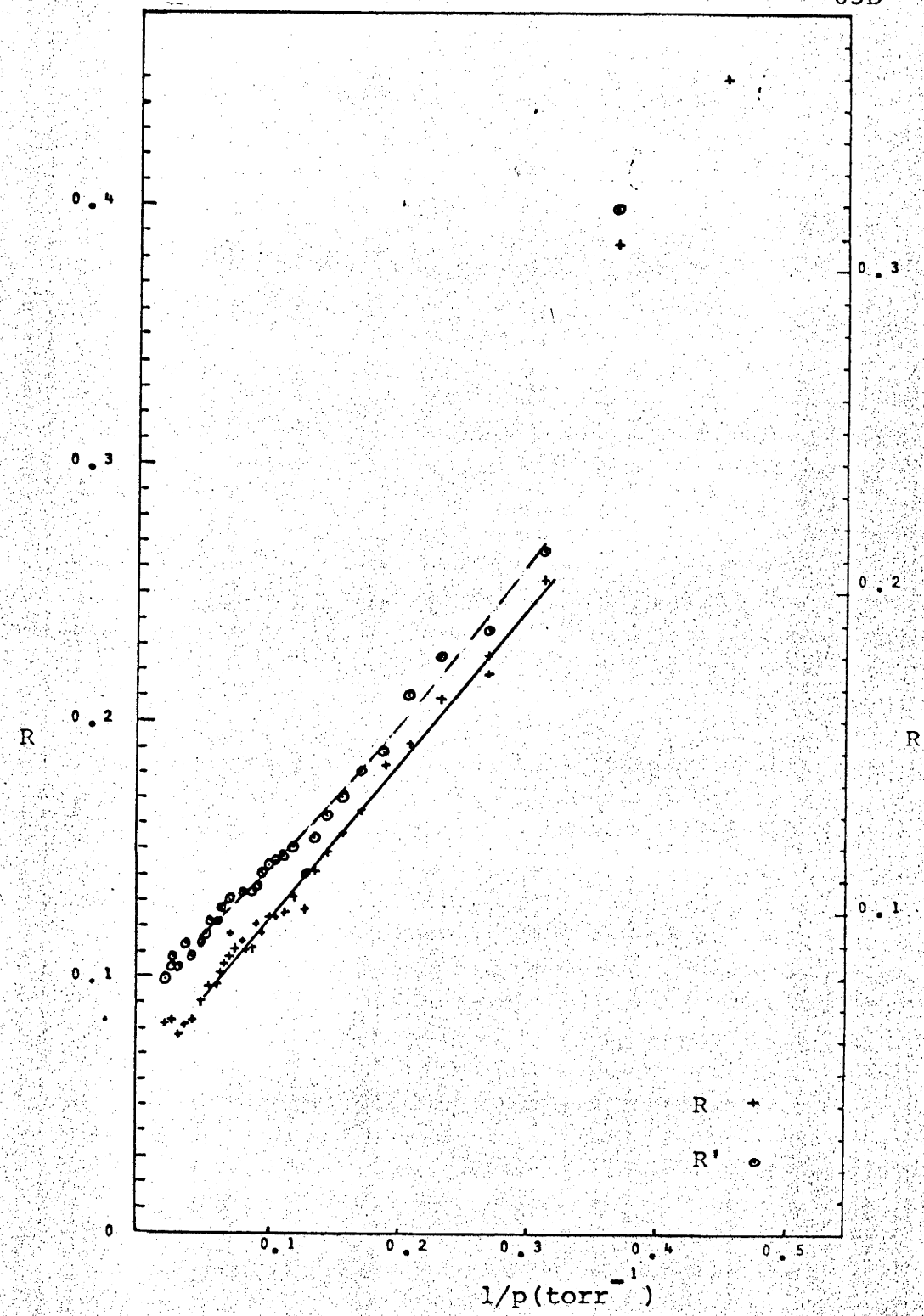

Fig. 5.4(d) - Caesium-Helium

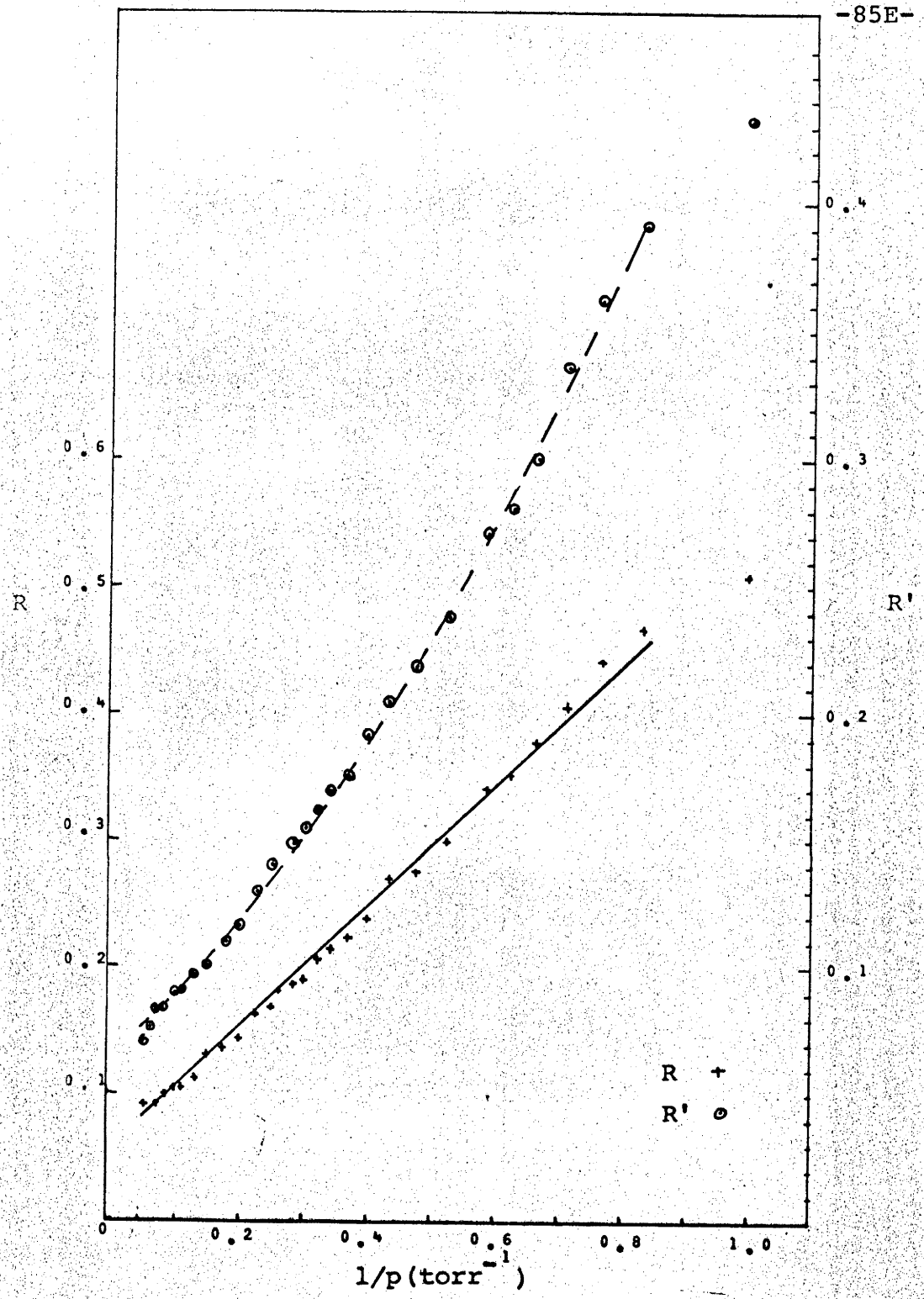

Fig. 5.4(e) - Caesium-Helium

(which are numbered to correspond to Figures 5.3). To allow for the approximations made in deriving equations (2.30) and (2.31) (regarding effects of caesium-caesium collisions at low pressure of inert gas, and population of $7D_{5/2}$ levels at high pressure) the pressure region in which R was close to a straight line was estimated by eye and the values of (R, 1/p) and (R', 1/p) in that region were fitted by computer to a straight line and to a parabola respectively. The computer technique used involved minimizing a function defined by the sum of the squares of the differences between the actual value and the fitted value at each point. The computer output provided values of the parameters in equations (2.46) and (2.50) and also estimates of their uncertainties.

The results obtained are given in Table 5.1. v_r is the relative velocity defined by equation (2.37) and T is the temperature of the upper part of the resonance cell. The accuracy of the cross-section was calculated from the scatter of experimental points given by the computer output.

The cross-sections obtained appear reasonable if one compares the cross-sections obtained by Krause[4]

	Cs-He		Cs-A			Cs-Kr	
Q_{12} ($\AA^2$)	20±10	40±7	8±1	6±2	8±1	12±3	19±7
Q_{21} ($\AA^2$)	20±10	40±10	-	6±4	-	3±2	13±7
Q_{23} ($\AA^2$)	13±1	16±1	16±1	35±2	29±2	39±3	57±5
Q_{32} ($\AA^2$)	3.3±0.3	3.9±0.3	4±1	11±1	2±1	8±1	26±3
T (^{o}K)	526	527	530	504	504	511	513
v_r ($m.s^{-1}$)	1690	1690	600	590	590	460	460

(Each column refers to a separate experimental run.)

Table 5.1 - Cross-sections for Caesium-Inert Gas Collisions

for potassium. Potassium is chosen because the energy defect involved (57 cm^{-1}) is not very different from the $8P_{1/2}$-$8P_{3/2}$ energy defect in caesium (82 cm^{-1}). The cross-sections given for potassium-inert gas collisions are of the order of 10 - 100 $Å^2$. Allowance should be made for the fact that potassium was in a 4P excited state while in this experiment the caesium is in an 8P state. A rough calculation using the formula for the mean value of the square of the radius of an electron in a one-electron atom[27] indicates that the gas-kinetic cross-section for the 8P level is about seventy times that for the 4P level. This would indicate an expected value of Q_{12} of the order of 700 - 7000 $Å^2$. (A similar calculation for the 7D levels indicates that the cross-section for the transfer $8P_{3/2} \rightarrow 7D_{3/2}$ (Q_{23}) should be about 1.8 times that for $7D_{3/2} \rightarrow 8P_{3/2}$ (Q_{32}).)

Krause[4] has obtained an interesting correlation between the cross-sections for alkali atom-inert gas excitation transfer collisions and for elastic scattering of electrons by inert gases[9]. He suggests that this indicates that the interaction may be essentially between an inert gas atom and a quasi-

free electron. A similar correlation has been attempted here in Figure 5.5. Using the Bohr model of the atom and the formula given by White[27] for the mean value of the radius of a one-electron atom in the 8P state, the velocity of this electron was calculated and from the electron cross-sections given by Massey and Burhop[9] the cross-sections at this velocity were estimated. These cross-sections are plotted in Figure 5.5 arbitrarily normalized so that the cross-sections for Argon coincide (i.e. Q_{12}). The cross-sections Q_{12} and Q_{23} are plotted and there seems to be some correlation in the case of $8P_{1/2} \rightarrow 8P_{3/2}$ transfers and perhaps also for $8P_{3/2} \rightarrow 7D_{3/2}$ transfers. (The cross-sections given for electron-inert gas collisions are not very precise at the velocity (0.38 √volts) calculated and were obtained by extrapolating the curves in Massey & Burhop.)

A notable feature of the cross-sections obtained is that $Q_{23}(8P_{3/2} \rightarrow 7D_{3/2})$ is greater than $Q_{21}(8P_{3/2} \rightarrow 8P_{1/2})$ for collisions with argon and krypton but the reverse is the case for collisions with helium. In this connection it may be noted that argon and krypton both exhibit the Ramsauer-Townsend effect[9] while helium

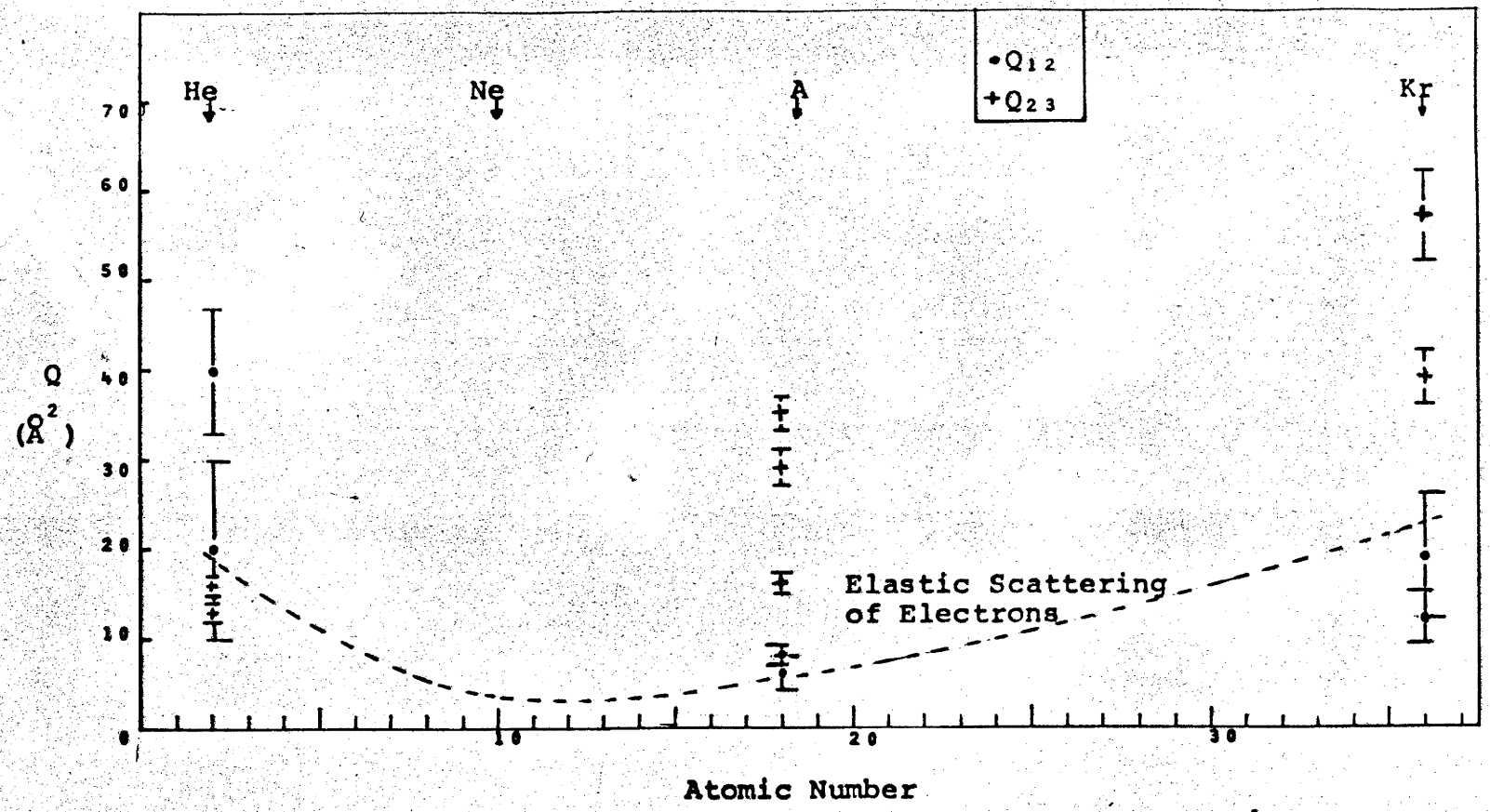

Fig. 5.5.- Comparison with Elastic Scattering of Electrons

does not. The feature of this effect is that, at a certain low electron velocity, argon and krypton become relatively transparent to electrons. This velocity is somewhere near that of the electron in the 8P or 7D levels of caesium. The occurrence of this effect is explained[28] by considering the zeroth order partial cross-section which is the only one of importance at low electron energies. For argon and krypton the phase shift η_0 approaches $s\pi$ (where s = 3,4 respectively) and so the cross-section becomes almost zero. ("Almost" because then the higher order partial cross-sections must be considered.) Helium presents a weak field in which s = 0 and sin η_0 tends to zero at the same rate as the associated electron energy by which it is divided to calculate the partial cross-section which, therefore, remains finite at low velocities.

There are, then, two links with the Ramsauer-Townsend effect which imply that the interaction in this experiment is one between an inert gas and a quasi-free valence electron.

5.4 SELECTION RULES FOR SENSITIZED FLUORESCENCE

It has been established (see for example Massey and Burhop[9], Chapter VII Section 10) that the

probability of an excitation transfer's occurring during a collision depends on a number of factors. For example, the greater the energy defect between the initial and final states, the smaller the probability of the transfer. On this basis, one would expect that the cross-sections for the excitation transfers $7D_{3/2} \overset{\leftarrow}{\rightarrow} 7D_{5/2}$, $8P_{1/2} \overset{\leftarrow}{\rightarrow} 8P_{3/2}$, and $8P_{3/2} \overset{\leftarrow}{\rightarrow} 7D_{3/2}$ would be greatest for the first, smaller for the second, and least for the third. No observations were made that would determine the first cross-section so the following discussion will be concerned only with the other two.

It was observed in the previous section that the cross-sections for the third process were larger than for the second except for the helium-caesium collisions where the opposite is the case. So at least for the case of helium, the energy resonance criterion holds though probably not as strongly as would be expected.

Winans[20] has proposed a partial selection rule for sensitized fluorescence. It is $\Delta J = 0$ where $J = J_A + J_B$, the vector sum of the individual angular momenta of the colliding atoms. Since, in

this case, the inert gas is not excited but remains in the ground state, then this rule simplifies to $\Delta J_A = 0$ where J_A is the angular momentum of the caesium atom.

Application of Winans' rule explains why the process $8P_{3/2} \overleftrightarrow{\rightarrow} 7D_{3/2}$ occurs but $8P_{1/2} \overleftrightarrow{\rightarrow} 7D_{3/2,5/2}$ and $8P_{3/2} \overleftrightarrow{\rightarrow} 7D_{5/2}$ apparently have lower probability since each of the last three violate $\Delta J_A = 0$. But the processes $8P_{1/2} \overleftrightarrow{\rightarrow} 8P_{3/2}$ and $7D_{3/2} \overleftrightarrow{\rightarrow} 7D_{5/2}$ clearly do violate the rule and quite clearly (for the former) or very probably (for the latter) do occur. The application of the partial selection rule must be therefore that if several alternative transitions are roughly equally probable considering the energy defects involved, then those transitions obeying the Winans selection rule are most probable.

Winans explains the derivation of his rule as being due to the formation of a quasi-molecule. He points out that most collisions between atoms are non-central (i.e. not head-on) ones and that the potential energy curves for these collisions are the same as for molecules in a state of high energy of rotation. The outstanding feature of such curves

is a maximum at comparatively large values of r, the interatomic distance. Hence the atoms may collide and be repelled without making a very close approach so that the individual angular momenta (J_A and J_B) remain good quantum numbers. Since the time of collision isless than the time for one revolution, only a partial quantization of J occurs so that the rule is only a partial one.

Since the relative velocity in the case of helium is larger than when argon and krypton are present then the quantization of J would be expected to be less effective for helium implying that the selection rule applies less for caesium-helium collisions than for caesium-argon or caesium-krypton collisions. The suggestion in the previous section that the interaction is actually with the valence electron, which is excited, substantiates the assertion that the interaction occurs at large inter-atomic distances.

In their paper[21], Chapman, Krause, and Brockman suggest a selection rule ΣJ_z = constant. This rule would permit all excitation transfers between the 8P and 7D levels to occur to some degree but

does not appear to apply in this case.

A further selection rule often invoked in thse situations is Wigner's rule which states that in an excitation exchange collision, of all possible transfers of energy with nearly equal energy defects, the most likely one is that in which the total resultant spin of the two-atom system remains unchanged[29]. Quite obviously this rule is not violated by any of the processes considered.

By considering the selection rules of Wigner and Winans together with the effect of energy defect and relative velocity of the colliding atoms it is, therefore, possible to give a qualitative explanation of the cross-sections obtained. It is also possible to show that the cross-sections are consistent with those obtained by other investigators and can be correlated with the cross-sections for elastic scattering of electrons by inert gases thereby implying that the interaction is primarily one between the buffer gas atoms and the valence electrons of the excited caesium atoms.

6. SUGGESTIONS FOR FURTHER RESEARCH

6.1 IMPROVEMENTS IN EXPERIMENTAL PROCEDURE

In the experiment described one improvement immediately suggests itself, the monitoring of fluorescent light at 6975 Å ($7D_{5/2} \rightarrow 6P_{3/2}$). By doing this it should be possible to calculate from equations (2.19) and (2.20) the cross-sections Q_{34} and Q_{43} for transitions between the two 7D levels. Then it should, in principle, be possible to work back through equations (2.18) and (2.19) to calculate Q_{23} and Q_{32}, the cross-sections for transfers between the levels $8P_{3/2}$ and $7D_{3/2}$. In this connection it should be stated here that this would eliminate the subjective judgement employed in the experiment when deciding which region of experimental data was to be fitted to the theoretical curve. The accuracy gained by this, however, would be less than it would theoretically be, due to using calculated values of k_{34} and k_{43} in the theoretical formula used to find k_{23} and k_{32} whose accuracy would of necessity be limited by the accuracy of k_{34} and k_{43}. Further, the theoretical formula for n_2/n_3 used to fit the data is less well constrained than that for n_3/ n_4 and consequently more difficult

to fit so that the parameters obtained would be less accurate. The accuracy will be even less when fitting the theoretical formula for n_1/n_2. Finally, the monitoring of the 6975 Å line would require a longer experiment with the attendant difficulties of keeping ambient conditions constant for a longer period. In short, the accuracy gained by being able to obtain values for k_{34} and k_{43} would be offset to some extent by added practical difficulties.

Another suggestion for further work involves the cross-sections for excitation transfers brought about by caesium-caesium collisions. The attempt to determine these (section 5.2) was abortive and should be easily rectified by use of a more suitable temperature measuring arrangement to provide a signal for the X axis of the recorder. By comparison with the results given by Krause[4] it is expected that these cross-sections should be larger than those obtained for collisions with inert gases.

As a check on the comparison made with elastic scattering of electrons, the experiment should be performed with neon and xenon as the buffer gases. The use of other gases such as methane which are

similar to the heavier inert gases in exhibiting the Ramsauer-Townsend effect might also be tried. Other gases such as nitrogen could be tried to determine quenching effects.

It is not to be expected that the type of experiment performed would yield much information regarding the nature of the interaction. Varying inert gas pressure should vary the frequency of collisions and little else. (Actually at high pressure there is a possibility of a different type of process, the three-body collision, occurring but it is reckoned that this did not occur to any significant extent.) If the temperature of the resonance cell were to be varied then the relative velocity of caesium atoms and inert gas atoms would be varied and the resultant variation of cross-section could be compared with theory such as that used in deriving the Landau-Zener formula for the probability of non-adiabatic transitions (see Hasted[29] p. 440). Such an experiment would involve carrying out the procedure described in section 4.9 for one particular buffer gas several times, each time with the resonance cell at a different temperature.

6.2 IMPROVEMENTS IN APPARATUS

The heart of the system is the resonance cell and the closely-coupled helium lamp. The close-coupling meant that a considerable fraction of the helium light was available for exciting caesium but this was at the expense of good temperature control of the resonance cell. It has already been pointed out that the upper part of the resonance cell was heated solely by the helium lamp and that the helium lamp did not operate constantly for long periods. Probably better control of temperature with a reduced illumination intensity would enhance the precision obtainable and be therefore a more desirable situation. A properly insulated oven for the upper part of the resonance cell with thermostatic temperature control should rectify this.

As stated in the previous paragraph, the helium lamp should have been better. Some improvement in this lamp is required and the possibility of using an r-f discharge should be looked into.

The caesium vapour density also ought to be better controlled. A properly insulated, thermostatically controlled oven is required here also.

The lower part of the resonance cell need not be so large and should be made as a small appendage to the upper part and should have reasonably thin walls.

Some improvements that could be made to the detection system are discussed in Appendix II. These include pulsing the helium lamp and thus eliminating the chopper, better cooling of the photomultiplier, and use of a more suitable grating. A less drastic method of cooling the photomultiplier than that referred to in Appendix II, and probably a more suitable one, is that described by Krause and Neville[31].

If the Philips 56CVP photomultiplier that had been ordered had arrived before the experiment was completed the dark current and its associated noise could have been reduced by a factor of about one hundred. This is possible because the 56CVP has a focussing electrode which enables the effective area of the photocathode to be controlled by varying its voltage. Hence the field between the cathode and first dynode can be adjusted so that electrons from only the illuminated part of the cathode can reach the first dynode and be subsequently amplified. A similar benefit is available with an I.T.T. F.W. 118G

photomultiplier which has a S-1 photocathode of small dimensions.

Precise adjustment of the monochromator was difficult at the best of times (section 4.8). A micrometer attachment such as that described by Combes and Gallagher[30] would make wavelength settings easier to obtain. It is claimed that with such an attachment, the monochromator could be adjusted to within 0.2 Å.

APPENDIX I

CAESIUM TRANSITION PROBABILITIES AND BRANCHING RATIOS*

Transition	Wavelength (Å)	Aij (10^6 sec^{-1})	Branching Ratio
$6P_{1/2} \rightarrow 6S_{1/2}$	8946	28.6	1
$6P_{3/2} \rightarrow 6S_{1/2}$	8524	32.4	1
$5D_{3/2} \rightarrow 6P_{1/2}$	30111	0.94	0.90
$\rightarrow 6P_{3/2}$	36140	0.11	0.10
$5D_{5/2} \rightarrow 6P_{3/2}$	34904	0.73	1
$7S_{1/2} \rightarrow 6P_{1/2}$	13591	6.23	0.35
$\rightarrow 6P_{3/2}$	14697	11.4	0.65
$7P_{1/2} \rightarrow 6S_{1/2}$	4594	2.12	0.29
$\rightarrow 5D_{3/2}$	13761	1.59	0.22
$\rightarrow 7S_{1/2}$	30960	3.52	0.49
$7P_{3/2} \rightarrow 6S_{1/2}$	4556	2.97	0.36
$\rightarrow 5D_{3/2}$	13426	0.13	0.016
$\rightarrow 5D_{5/2}$	13605	1.10	0.13
$\rightarrow 7S_{1/2}$	29317	4.05	0.49
$6D_{3/2} \rightarrow 6P_{1/2}$	8763	12.7	0.82
$\rightarrow 6P_{3/2}$	9211	2.66	0.17
$\rightarrow 7P_{1/2}$	121507	0.090	0.0058
$\rightarrow 7P_{3/2}$	155763	0.0086	0.00056

Transition	Wavelength (Å)	Aij (10^6 sec^{-1})	Branching Ratio
$6D_{5/2} \rightarrow 6P_{3/2}$	9174	15.2	0.996
$\rightarrow 7P_{3/2}$	145985	0.063	0.004
$8S_{1/2} \rightarrow 6P_{1/2}$	7611	2.04	0.21
$\rightarrow 6P_{3/2}$	7946	3.60	0.37
$\rightarrow 7P_{1/2}$	39200	1.38	0.14
$\rightarrow 7P_{3/2}$	42194	2.62	0.27
$8P_{1/2} \rightarrow 6S_{1/2}$	3889	0.578	0.19
$\rightarrow 5D_{3/2}$	8921	0.513	0.17
$\rightarrow 7S_{1/2}$	13941	0.364	0.12
$\rightarrow 6D_{3/2}$	32051	0.733	0.24
$\rightarrow 8S_{1/2}$	71839	0.835	0.27
$8P_{3/2} \rightarrow 6S_{1/2}$	3876	0.940	0.25
$\rightarrow 5D_{3/2}$	8859	0.045	0.012
$\rightarrow 5D_{5/2}$	8933	0.397	0.11
$\rightarrow 7S_{1/2}$	13784	0.565	0.015
$\rightarrow 6D_{3/2}$	31230	0.086	0.023
$\rightarrow 6D_{5/2}$	31656	0.746	0.20
$\rightarrow 8S_{1/2}$	67843	0.956	0.26
$7D_{3/2} \rightarrow 6P_{1/2}$	6725	6.54	0.65
$\rightarrow 6P_{3/2}$	6985	1.31	0.13

Transition	Wavelength (Å)	Aij (10^6 sec^{-1})	Branching Ratio
$7D_{3/2} \rightarrow 7P_{1/2}$	23354	1.53	0.15
$\rightarrow 7P_{3/2}$	24384	0.37	0.037
$\rightarrow 8P_{1/2}$	294985	0.017	0.0017
$\rightarrow 8P_{3/2}$	389105	0.0017	0.0002
$\rightarrow 4F_{5/2}$	1576	0.33	0.033
$7D_{5/2} \rightarrow 6P_{3/2}$	6975	7.89	0.75
$\rightarrow 7P_{3/2}$	24260	2.23	0.21
$\rightarrow 8P_{3/2}$	359712	0.013	0.0012
$\rightarrow 4F_{5/2}$	1597	0.016	0.0015
$\rightarrow 4F_{7/2}$	1597	0.33	0.032

*Adapted from references (14) and (17)

APPENDIX II

NOISE AND THE DETECTION OF WEAK SIGNALS

The light signals ovserved were very weak (especially the 8933 Å line). For example the amplifier had to be operated at full (100 db) amplification to observe variation of the 8933 Å line, at 90-100 db for the 8921 Å line, and at 75-85 db for the 6985 Å line. Part of the reason for low intensity was the grating used which was meant for visible radiation. The low sensitivity of the photomultiplier (quantum efficiency ~0.35% at all of the wavelengths) was also a contributing factor.

At such low signal levels, the presence of noise becomes a very real threat to the success of an experiment. Without some special signal recovery technique, such as the phase-sensitive detector method used, this experiment would not have been able to be carried out.

Some of the sources of noise that could have affected the experiment will now be considered.

Electromagnetic pickup is always a possibility. In this case the Beckman power supply used for the

helium discharge was very likely to be a source of noise. This was placed on the far side of the apparatus away from the detection equipment so as to minimize its effects. The use of double-shielded coaxial cable for the leads between various parts of the detector would also have reduced electromagnetic noise. Another source that was not suspected until it broke down was the hot-air blower mentioned earlier. When it was discarded the output level of the low-noise amplifier dropped from 0.3V to 0.1V. Another precaution employed was the use of short cables wherever possible.

The chopper was powered by a domestic fan synchronous motor which may have been a source of some noise. More important was the fact that this motor was mounted on the front of the monochromator and caused low frequency vibrations which could just be detected by placing one's hand on the monochromator. Since the photomultiplier housing was also mounted on the monochromator a possibility of microphonic noise existed.

An important noise source was the helium discharge. Its effects have already been pointed out

in section 5.1.

Since the resonance cell was kept at an elevated temperature (~500^{o}K) it emitted black-body radiation which was modulated by the chopper together with the required signal and thus will not be discriminated against by the detection system. So improvement of the signal-to-(this) noise ratio was not possible by means of the system used. One way to remedy this is to use a radiofrequency helium lamp modulated at some low frequency[22] (~100 Hz) to excite the fluorescence. This would enable the chopper wheel to be dispensed with altogether thus removing two noise sources.

Another cause of noise was the existence of earth loops. These are complete circuits formed by earth wires which are able to carry stray currents which cause noise. Careful earthing was required to reduce this source to a low level so that the weakest signals were detectable. The optimum earthing arrangement was found by trial and error. Important considerations were the provision of one central earth point and the connection of the earthed shield of coaxial cable at only one end in some cases.

Summaries of the types of noise limiting the sensitivity of photomultipliers are readily available in the literature supplied by manufacturers.[23,24] The main noise sources are dark current and its associated shot noise (due to randomness of the dark current emission), gain variations, and Johnson noise in the load resistor. In the case of photomultipliers, the last mentioned effect is usually less than other effects.

A dynode chain was designed according to the manufacturer's recommendations. The design is referred to as "linear simple high gain". Since gain variations are most important in the cathode-first dynode region a Zener diode stabilized voltage was used for this stage. The rest of the chain was designed so that the chain current was more than ten times the mean anode current to minimize gain variation in this part of the chain.

Cooling of the photomultiplier was employed to reduce the dark current which may otherwise be considerable for an S-1 type photocathode. This also reduces the dark current shot noise. It was apparent that better cooling would have been desirable. For example the method used by Wiggins and Earley[25] in

which a photomultiplier was immersed in a dewar of liquid nitrogen would have reduced the dark current even more.

Simple precautions were taken against stray currents due to ohmic leakage. The photomultiplier tube was thoroughly cleaned with methyl alcohol to remove grease and dirt and silica-gel was placed inside the photomultiplier housing to reduce the humidity.

The major component of the system to discriminate against noise is the phase-sensitive detector or lock-in detector. The operation of such a system is described in the literature[26]. Basically the D.C. signal is converted to A.C. by chopping at a frequency high enough to avoid the low frequency region where flicker (1/f) noise of the electronic instruments is considerable. This results in a signal that has a reasonably constant frequency (depending on the constancy of the chopping) and narrow bandwidth which is then amplified to a level high enough to operate the detector. This is achieved by use of a low-noise amplifier which has a narrow, selectable bandwidth at the chopping frequency and

thus discriminates against noise of frequencies outside this bandwidth. Finally a detector is used to convert the signal back to D.C. The reference signal for the detector is provided by the same chopper that chops the signal so the name homodyne amplifier is sometimes used to describe the system. To reduce noise as much as possible, the detector requires a very narrow bandwidth which has a lower limit determined only by the rapidity with which the observed signal varies. This bandwidth is adjusted by use of an R-C time constant. Hence in this experiment it was possible to discriminate against all but the required signal and thermal radiation from the resonance cell. Probably some photomultiplier shot noise associated with the dark current and the signal in the correct frequency band was also present in the output. It is also possible that the chopping frequency used (142 Hz) was not high enough to avoid flicker noise properly and that a higher chopping frequency would have been more desirable.

Mathematically, the output of the phase-sensitive detector is the product of the input signal

and the reference signal. If the latter is v sin ωt and the former has a component V sin $(\omega t + \alpha)$ then a D.C. voltage will appear across the load resistor proportional to V cos α plus two other terms with a frequency of 2ω. Any noise voltages in the signal which are not coherent with the reference signal will produce A.C. voltages across the load resistor at various beat frequencies. If all the A.C. voltages are filtered out then the noise content of the output will depend only on the time constant of the system which can be made as long as required subject to the limitation mentioned in the previous paragraph. Response of the system to noise bands centred on odd harmonics of the reference system is practically eliminated by limiting the band-width of the low-noise amplifier. By adjusting the phase α, the signal-to-noise ratio can thus be optimized. If the signal and reference voltages are not sinusoidal, then they can be analysed into their Fourier components and the same argument applies.

REFERENCES

(1) Boeckner, C: J. Res. Nat. Bur. Stand. (U.S.A.) 5, 13 (1930)

(2) Rabinowitz, P, Jacobs, S, and Gould, G: Appl. Optics (U.S.A.) 1, 513 (1962)

(3) Mitchell, A.C.G., and Zemansky, M.W.: Resonance Radiation and Excited Atoms, (Cambridge University Press, London 1934)

(4) Krause, L: Appl. Optics (U.S.A.) 5, 1375 (1966)

(5) McGillis, D.A. and Krause, L: Canad. J. Phys. 46, 1051 (1968)

(6) Holstein, T: Phys. Rev. (U.S.A.) 72, 1212 (1947): Phys. Rev. (U.S.A.) 83, 1159 (1951)

(7) Adapted from Gould, G: Proceedings of the Third International Congress on Quantum Electronics (Columbia University Press, New York, 1964) p. 461.

(8) Moore, C.E.: Atomic Energy Levels Vol. 3 (National Bureau of Standards Circular 467, Washington 1958)

(9) Massey, H.S.W. and Burhop, E.H.S.: Electronic and Ionic Impact Phenomena, (Oxford University Press, London 1952) pp. 9, 10.

(10) Fastie, W.G.: J. Opt. Soc. Amer., 42, 641 (1952)

(11) Taylor, J.B. and Langmuir, I: Phys. Rev. (U.S.A.) 51, 754 (1937).

(12) See Reference (3), p. 31

(13) Gallagher, A: Phys. Rev. (U.S.A.) 172, 88 (1968)

(14) Allen, L. and Heavens, O.S.: Phys. Letters 2, 35 (1962)

(15) Seiwert, R.: Ann. Physik 18, 54 (1956)

(16) Handbook of Chemistry and Physics - 45th Ed. (1964-5) (The Chemical Rubber Company, Cleveland, Ohio)

(17) Smith, W.V. and Sorokin, P.P.: The Laser (McGraw-Hill, 1966) p.202

(18) Laidler, K.J.: Reaction Kinetics: Volume 1 - Homogeneous Gas Reactions, (Pergamon Press, Oxford, 1963)

(19) Kondrat'ev, V.N.: Chemical Kinetics of Gas Reactions (translated from Russian by Crabtree, J.M. and Carruthers, S.N., Pergamon Press, Oxford, 1964)

(20) Winans, J.G.: Rev. Mod. Phys. (U.S.A.) 16, 175 (1944)

(21) Chapman, G.D., Krause, L., and Brockman, I.H.: Canad. J. Phys., 42, 535 (1964)

(22) Jacobs, S., Gould, G., Rabinowitz, P.: Phys. Rev. Letters (U.S.A.) 7, 415, (1961)

(23) E.M.I. Photomultiplier Tubes (E.M.I. Electronics Ltd., Valve Division) (Brochure Ref.: 30M/6-67 (PMT) Issue 1)

(24) Phototubes and Photocells (Amalgamated Wireless Valve Company Pty. Ltd., Sydney) (Publication No. PP1)

(25) Wiggins, C.S. and Earley, K.: Rev. Sci. Instrum. (U.S.A.) 33, 1057 (1962)

(26) Moore, R.D., and Chaykowski, O.C.: Tech. Bull. 109, Princeton Applied Research Corporation 1963

(27) White, H.E.: Introduction to Atomic Spectra (McGraw-Hill, 1934) (p.69)

(28) See Reference (9), p. 113

(29) Hasted, J.B.: Physics of Atomic Collisions (Butterworths, London, 1964) p. 450

(30) Combes, L.S. and Gallagher, C.C.: Appl. Optics (U.S.A.) 7, 857 (1968)

(31) Krause, L. and Neville, R.A.: Rev. Sci. Instrum. (U.S.A.) 34, 698 (1963)